GEOSCIENCE AUSTRALIA

Australian Government
Geoscience Australia

3D Geological Modelling and Petroleum Prospectivity Assessment in Offshore Frontier Basins using GOCAD™: Capel and Faust Basins, Lord Howe Rise

Record
2011/01

GeoCat # 70174

K.L. Higgins, T. Hashimoto, R. Hackney, P. Petkovic and P. Milligan.

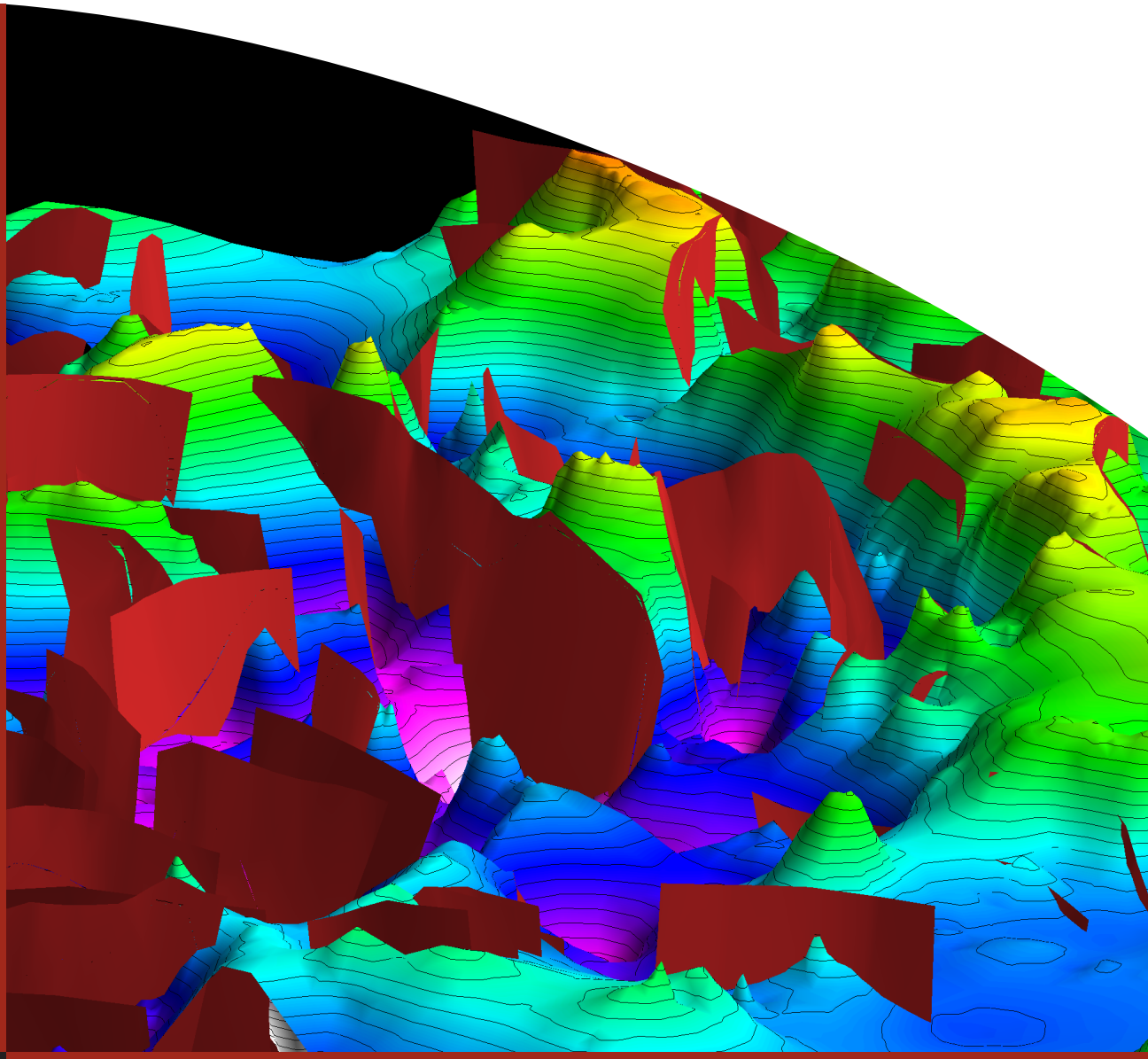

APPLYING GEOSCIENCE TO AUSTRALIA'S MOST IMPORTANT CHALLENGES

3D Geological Modelling and Petroleum Prospectivity Assessment in Offshore Frontier Basins using GOCAD™: Capel and Faust Basins, Lord Howe Rise

GEOSCIENCE AUSTRALIA
RECORD 2011/01

by

K.L. Higgins, T. Hashimoto, R. Hackney, P. Petkovic and P. Milligan.

Australian Government
Geoscience Australia

Department of Industry, Tourism & Resources
Minister for Resources and Energy: The Hon. Martin Ferguson, AM MP
Secretary: Mr Drew Clarke

Geoscience Australia
Chief Executive Officer: Dr Chris Pigram

ISSN 1448-2177
ISBN 978-1-921781-68-1
978-1-921781-69-8 (CD-ROM)
GeoCat # 70174

Bibliographic reference:

Higgins K.L., Hashimoto T., Hackney R., Petkovic P. and Milligan, P., 2011. 3D Geological Modelling and Petroleum Prospectivity Assessment in Offshore Frontier Basins using GOCAD™: Capel and Faust Basins, Lord Howe Rise. Geoscience Australia Record 2011/01

Contents

1. Executive Summary

The Capel and Faust basins are located over the northern part of the Lord Howe Rise, a large offshore frontier region containing a number of basins with untested petroleum prospectivity. Recent data acquisition by Geoscience Australia has significantly improved geological knowledge of these basins. Given the diversity of acquired data, comparative sparseness of data coverage, lack of deep drilling control, and complexity of geological structure, effective data integration and analysis methods were essential for a meaningful geological interpretation of the Capel and Faust basins. By using the 3D visualisation and modelling environment provided by GOCAD™, the datasets were captured, processed and interpreted to create an integrated 3D model that enabled key geological and prospectivity questions to be answered. This report summarises the construction methodology and the resulting geological and prospectivity implications of the Capel-Faust 3D geological model.

The results of the 3D model indicate that the Capel-Faust region is structurally complex, composed of a number of graben and half-graben depocentres, rather than two large basins, as was previously defined. The central and northwestern areas contain the largest depocentres, with dimensions of up to 150 km long and 40 km wide. These depocentres contain sediment thicknesses sufficient for hydrocarbon generation, with a maximum thickness of 3.7 s TWT (~6.7 km). The highly compartmentalised architecture of the depocentres could inhibit long-distance lateral migration of any hydrocarbons away from the potential kitchen areas in the deeper parts of the depocentres, but 3D modelling has improved visualisation of possible migration pathways and trapping structures. The overall depocentre orientations across the study area show zonation with eastern and western ~NW-trending depocentres and centrally located ~N-trending depocentres. This structural zonation has been attributed to oblique extension on a strong pre-existing NW-trending fabric, as indicated by interpreted basement terranes (such as the New England Orogen) and regional trends in datasets.

The rift depocentres formed as part of the final breakup of eastern Gondwana, which started in the Early Cretaceous and culminated in the opening of the Tasman Sea (c. 85–52 Ma). Rifting took place in two main phases, which were followed by post-rift thermal subsidence. The first rifting event, the Syn-rift 1 phase (Early Cretaceous-Cenomanian) deposited up to 2.5 s TWT (~5 km) of sediment in centrally located N-trending depocentres. The second rifting event, Syn-rift 2, (Cenomanian-Campanian) deposited up to 1.5 s TWT (~2.8 km) of sediment in NW-trending depocentres in the NW part of the study area. Rifting was probably terminated due to the opening of the Middleton and Tasman Sea basins at this latitude during the Campanian–Maastrichtian. Subsequent deposition is characterised by a post-rift sag succession with up to 1.7 s TWT (~2.3 km) of sedimentation focused over pre-existing depocentres. Seismic character analysis, regional tectonic reconstructions and analogue basin studies suggest the likely presence of potential source rocks in the pre-rift, Syn-rift 1 and Lower Syn-rift 2 successions, potential reservoirs in the Upper Syn-rift 2 and Lower Post-rift successions, and regional seals in the Upper Post-rift section. Major structuring events have interrupted deposition during syn-rift and post-rift phases, resulting in the formation of potential trapping structures and possibly encouraging hydrocarbon migration.

2. Introduction

This report outlines the methodology employed in the building of the Capel-Faust 3D geologic model, and the implications of modelling results. Associated reports (Colwell et al., 2010; Petkovic, 2010; Hackney, 2010) provide further detail on other aspects of the geological and prospectivity assessment of the Capel and Faust basins.

The Capel and Faust basins are located over the northern part of the Lord Howe Rise (LHR; Figure 1), a large continental fragment that was rifted from eastern Australia in the Cretaceous during the opening of the Tasman Sea Basin (Hayes and Ringis, 1973; Gaina et al., 1998). These frontier basins were identified as of potential interest to the petroleum exploration industry under the Australian Government's New Oil (2003–2007) and Offshore Energy Security (2006–2011) programs.

The Lord Howe Rise extends 1600 km from the Kenn Plateau in the north to the Challenger Plateau in the south, and is up to 600 km wide (Figure 1). It contains a number of rift basins that are likely to have petroleum potential (Stagg et al. 1999; Blevin, 2001; Willcox et al., 2001; Van de Beuque, 2003; Norvick et al., 2008). Of these basins, the Capel and Faust basins were assessed as being the most promising with thick sediments and large structures identified on three pre-existing seismic lines (regional seismic survey GA-206). The two basins cover an area of approximately 210 000 km^2 in water depths of 1500–3000 m. The sparseness and generally poor quality of existing seismic data, and the lack of well control, with the exception of one shallow DSDP hole (DSDP 208, total depth of 594 m), precluded the petroleum prospectivity assessment of these basins until recent data acquisition by Geoscience Australia.

In 2006, Geoscience Australia completed the joint Australian–French Australia–Fairway Basin Bathymetry and Sampling Survey (AUSFAIR MD153), acquiring ship-track swath bathymetry, sub-bottom profiler, gravity and magnetic data, as well as five dredge hauls and seven giant CALYPSO piston cores (Colwell et al., 2006). In late 2006 and early 2007, the Capel–Faust GA-302 survey acquired approximately 6 000 km of 106-fold 2D seismic data along 23 lines, with a typical spacing of 15–30 km (Kroh et al., 2007). Ship-track gravity and magnetic data were also collected. The GA-2436 survey using the vessel RV *Tangaroa* in late 2007 acquired a number of dredge samples and approximately 24 000 km^2 of high-quality multibeam bathymetry and 11 000 line km of shipboard gravity and magnetic data, with a line spacing of 3–4 km over the central part of the Capel and Faust basins, (Heap et al., 2009; Figure 2).

Given the diversity of acquired data, the comparative sparseness of data coverage, despite the new data acquisition, and the structural complexity of the basins, effective data integration and analysis methods were required. By using the 3D visualisation and modelling environment provided by GOCAD™, the diverse datasets were captured, processed and interpreted to create an integrated basin model that enabled key geological and prospectivity questions to be answered. 3D gravity modelling was also integrated in the workflow (Figure 3) as a quality-control mechanism for the seismic interpretation, the main input data to the GOCAD™ model, and is discussed in Petkovic (2010).

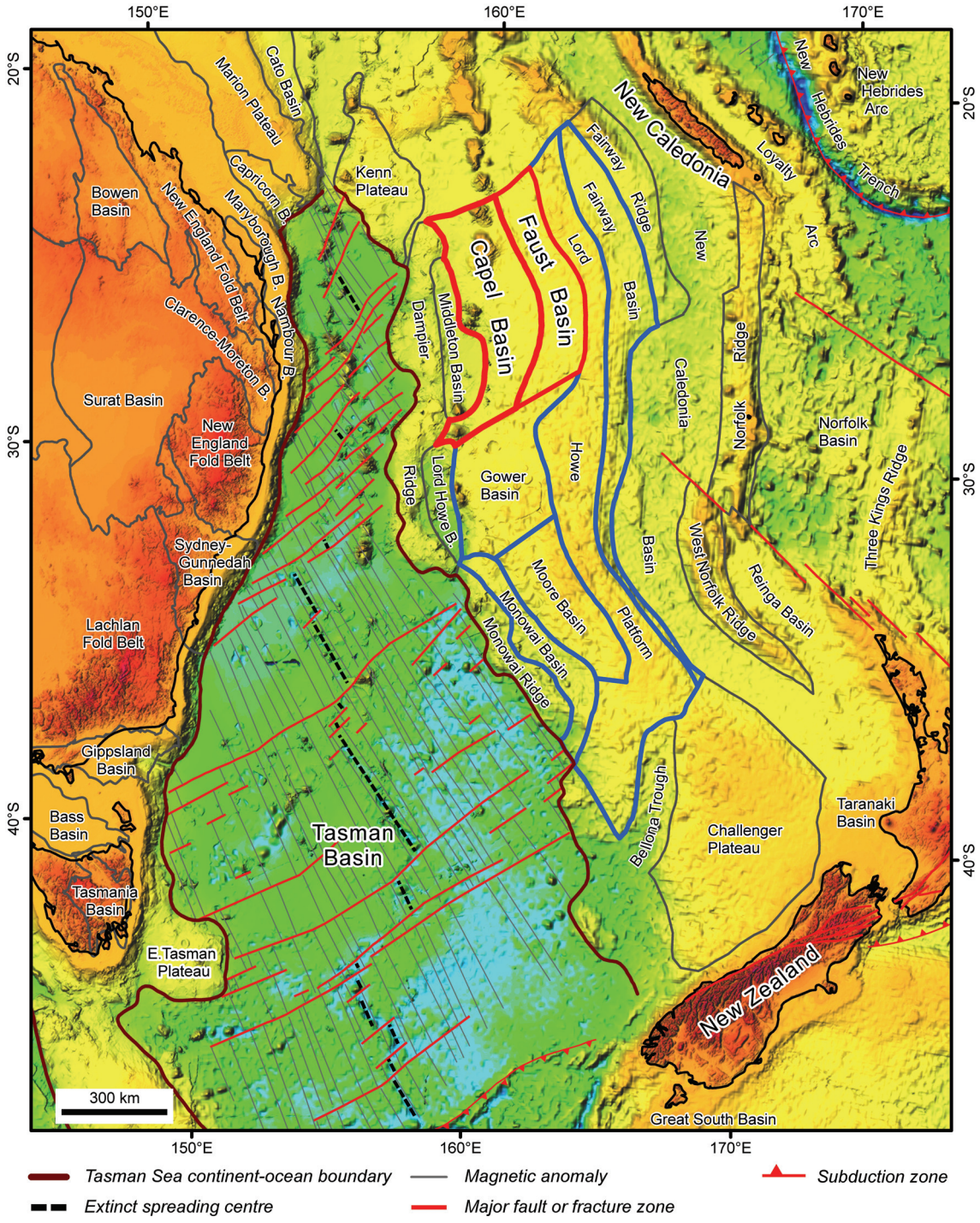

***Figure 1**: The location of the Capel and Faust basins (red outlines) with major tectonic elements of the Lord Howe Rise outlined in blue on a bathymetric image (Hashimoto et al., 2008).*

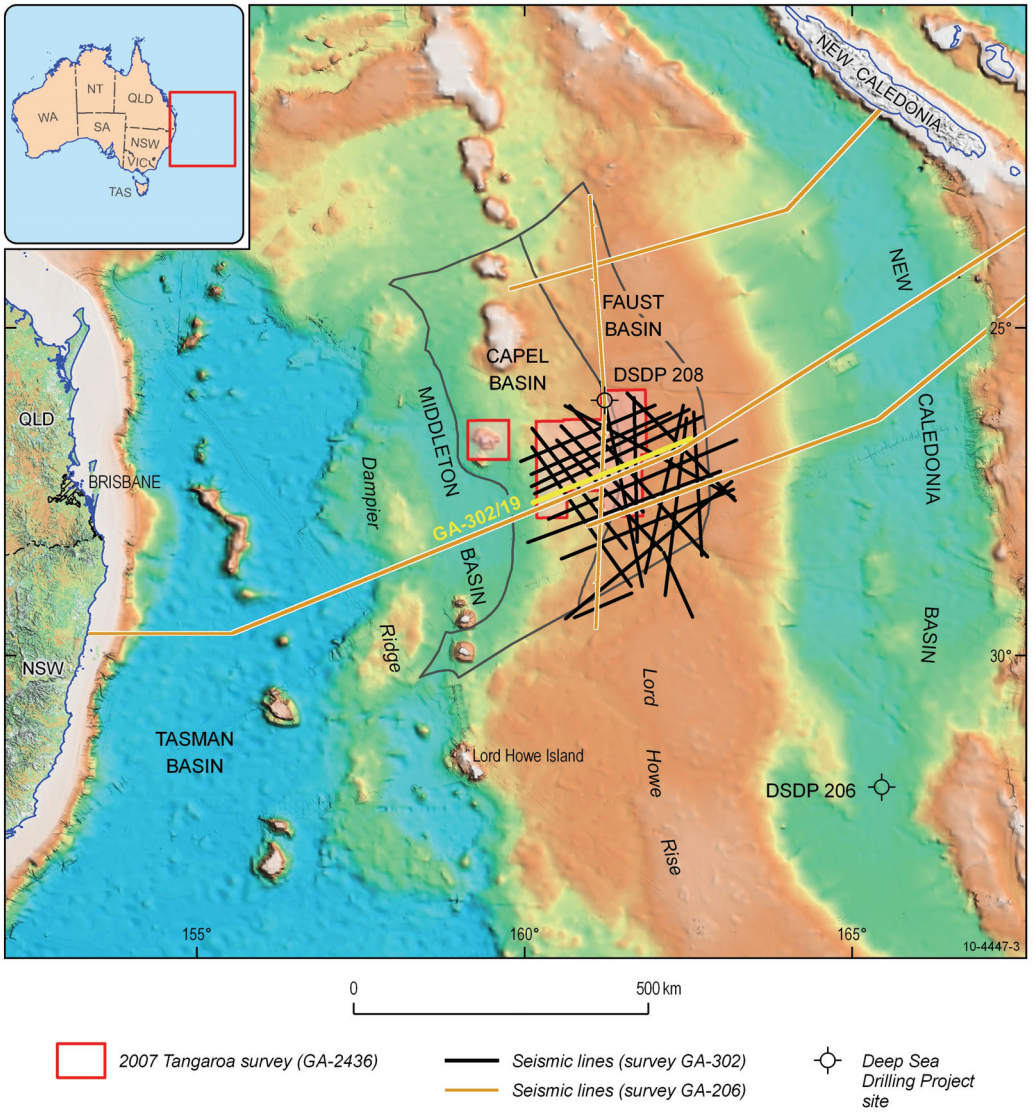

Figure 2: *The location of data acquisition by Geoscience Australia in the Capel and Faust area with DSDP holes on a bathymetric image (Colwell et al., 2010). Line location of seismic line GA-302/19 (Figure 12) is highlighted in yellow.*

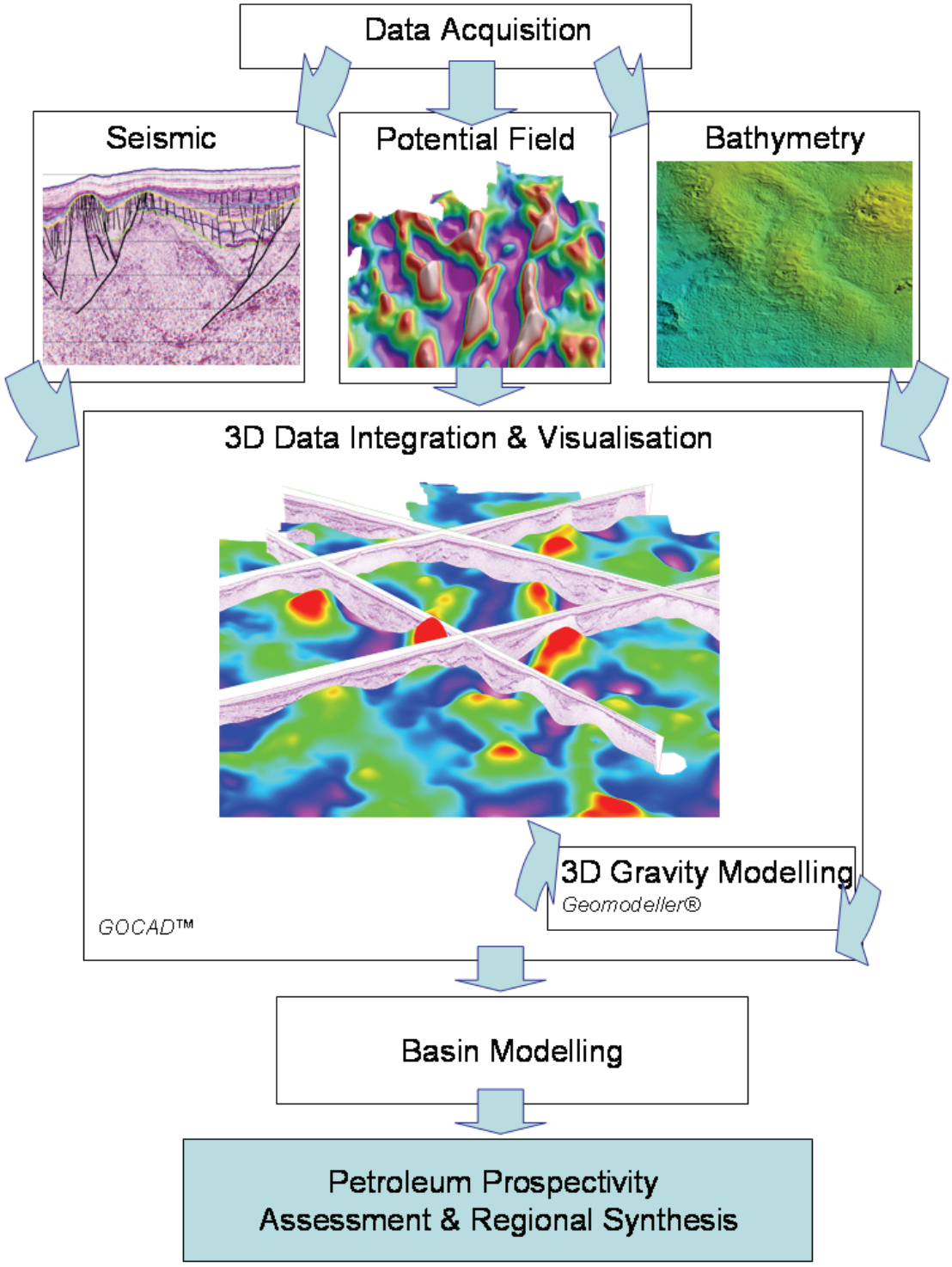

Figure 3: *The Capel and Faust basin analysis workflow using 3D modelling and visualisation as a key component for prospectivity analysis.*

3. Software and Datasets

3.1 SOFTWARE AND PROJECT STRUCTURE

3.1.1 Paradigm GOCAD™ Base Module

GOCAD™ is a 3D visualisation and modelling software program both developed and sold by Paradigm. The program allows the integration of diverse datasets including seismic, geological interpretation, potential field, bathymetry, velocity and well data, in a 3D environment. It also enables 3D model building; such as horizon and fault surface creation, with a variety of manipulation and interpolation tools available to the user. This flexibility led to the software being appropriate for the Capel-Faust data and 3D model. GOCAD™ Base Module 2009, 2.5.2 and 2.6.1 were used for most of the processes outlined in this report and the project properties are listed below. Plug-ins from the GOCAD™ Consortium (http://gocad.ensg.inpl-nancy.fr/www/consortium/index.xhtml), scripts and wizards from Jigsaw Geoscience (http://www.jigsawgeoscience.com.au/) and Mining Utilities from Mira Geoscience (http://www.mirageoscience.com/) were also utilised during the model building process.

Further information about the GOCAD™ software and system requirements can be accessed via the Paradigm website (http://www.pdgm.com/products/gocad.aspx).

3.1.2 ParaViewGeo

ParaViewGeo is an open source visualisation software package allowing the integration and visualisation of 3D models. The software has the ability to read over 50 different file formats, including GOCAD™ objects and can handle terabyte size datasets. ParaViewGeo version 1.4.15 (Win 32) has been included in the data package for clients without access to GOCAD.

Further information about the ParaViewGeo software, downloads and system requirements can be accessed via this website: http://paraviewgeo.mirarco.org/index.php/Main_Page.

3.1.3 3D Models

LHR_Capel_Faust_3D_Time
LHR_Capel_Faust_3D_Depth
GOCAD™: 2.5.2 Base Module
Projection: WGS84 UTM57S
Area: 300 by 400 km
Area Units: Meters
Depth Unit: Meters
Time Unit: Milliseconds
Depth Axis Positive Values: Downward
Recommended Vertical Exaggeration for Viewing: 5

3.1.4 Project Structure

LHR_Capel_Faust_3D_Time/Depth
Favourites
Basic Data
Bathymetry:
All basic datasets (surfaces and images) for the region capturing both local and regional seafloor topography. Bathymetry images are draped onto seafloor surfaces to provide finer detail.

Capel_Faust_Bathymetry_Image_100m
Capel_Faust_Bathymetry_Surface
Regional_Bathymetry_2km

Cultural:
Datasets containing cultural information including the Exclusive Economic Zone (EEZ) and treaty boundaries with neighbouring countries. Location information such as the Australian coastline and the area of interest is also included.

Australian_Coastline
Australian_EEZ
Australian_Continental Shelf
Capel_Faust_Region
Treaty_Boundary_France_Aus
Treaty_Boundary_NewZealand_Aus

Potential field:
Datasets of processed potential field data (magnetic and gravity). Images are draped onto surfaces to provide finer detail. Major trends in these datasets have been highlighted via worming of the data and associated simplified derived orientations of the worms. These datasets were utilised for the creation of the structural interpretation model of the region

Gravity
- Gravity_Image
- Gravity_Surface
- Worms
  - Derived Orientations
  - Gravity_Worms

Magnetic
- Magnetics_Image
- Magnetics_Surface
- Worms
  - Derived_Orientations
  - Magnetic_Worms

Seismic:
Key seismic surveys over the Capel-Faust region.

GA-206
S302

Wells:
Key wells in the Capel-Faust region for interpretation ties, seismic analysis and stratigraphic correlations. Data includes age markers and well logs.

DSDP_Locations
DSDP_208_Well

Depth Conversion (Depth model only)
Velocity model voxet constructed from velocity algorithms in the Capel-Faust region and used to convert time objects, such as seismic interpretation, into depth.

Velocity _Model

Note: In the LHR_Capel_Faust_3D_Depth model objects that have been converted from time to depth are identified by having the prefix “depth_” in the objects name.

Interpretation

1_ Blanket_Model:

3D model of the Capel-Faust region constructed so that all key seismic horizon surfaces are regionally extensive. These surfaces feed into 2D surface analysis (particularly fault displacement), geohistory modelling and potentially depth conversion processes. Model includes all key seismic horizon surfaces, interpretation points, fault surfaces, fault displacement surfaces, major and minor fault seismic curves and fault tops and bottoms curves.

Curves
PointsSets
Surfaces

2_Geological_Model:

3D model of the Capel-Faust region derived from the "blanket model" but constructed so that all key seismic horizon surfaces honour geological relationships, for example terminating onto features such as basement highs. These surfaces are not regionally extensive and feed into 3D geological analysis and visualisation of the Capel-Faust region. Model includes all key seismic horizon surfaces, interpretation points and fault surfaces.

PointsSets
Surfaces

3_Structure_Model:

All datasets related to the construction of a 3D structure model representing major fault zones for the region. This includes interpreted trends based on potential field, seismic and bathymetric data as well as trends derived from processed potential field data (such as worms and associated derived orientations). Fault displacement surfaces constructed from key horizon surfaces are also included and represent changes in the tectonostratigraphic development of the region over time.

Fault_Curves	Major and minor faults as interpreted from seismic
Fault_Displacement	Surfaces representing fault displacement for each horizon surface. Fault tops and bottoms
Fault_Orientation_Data	
Fault_Surfaces	Final fault surfaces representing interpreted major fault zones based on basic datasets.
Fault_Trends	Fault_Curves – curves defining interpreted fault zones based on basic datasets. Base datasets for constructing final fault surfaces. Major_Faults Minor_Faults Interpreted_Bathymetric_Trends Interpreted_Gravity_Trends Interpreted_Magnetic_Trends

4_Horizons:

All horizon datasets for the Capel_Faust region, encompassing the original interpretation data and constructed surfaces, as well as the final "blanket" and "geological model" datasets.

PointsSets
Surfaces

Views
Views are provided in the finalised time and depth projects to assist the end user to interrogate the model. The views are named according to the central dataset focus of the view. The end user is also able to create new views to suit their own specific purposes.

Capel_Faust_Region
Horizon_PointsSets
Magnetic_Worms
Gravity_Worms
Bathymetry
Regional_Overview
Faults
2D_Faults_Major_and_Minor
Gravity
Magnetics
Regional_Bathymetry
Horizon_Surfaces_Basement
Seismic_GA-206
Seismic_S302
DSDP_208

3.2 CULTURAL DATA

3.2.1 Australian Maritime and Treaty Boundaries

The Australian Maritime and Treaty Boundaries (AMB) is a dataset depicting the limits of Australia's maritime jurisdiction as set out under United Nations Convention on the Law of the Sea (UNCLOS) and relevant domestic legislation. To this extent, AMB provides a digital representation of the outer limit of the 12 nautical mile territorial sea, the 24 nautical mile contiguous zone, the 200 nautical mile EEZ and Australia's Continental Shelf, as well as the 3 nautical mile coastal waters. Where Australia has agreements with neighbouring countries these treaty lines are also included in the data.

The dataset has been compiled by Geoscience Australia in consultation with other relevant Australian Government agencies including the Attorney-General's Department, the Department of Foreign Affairs and Trade as well as the Australian Hydrographic Office.
Australia's maritime boundaries are computed from the territorial sea baseline, which has been mapped by Geoscience Australia using the most reliable information available at the time it was compiled. It should be noted that the territorial sea baseline supplied in AMB is not intended to be a comprehensive coastline dataset and only contains features relevant to maritime boundary determination. Basepoints that generate the zone boundaries are supplied in separate files.

Other data included in AMB are the 'Scheduled Area' boundaries of the Petroleum (Submerged Lands) Act 1967 (Commonwealth), individual line and point files depicting maritime boundary agreements with neighbouring countries, and polygon data of the various maritime zones supplied primarily for mapping purposes.

AMB data is clearly attributed, providing information about the source material used to determine the baseline and linking the baseline with the various limits. The data are available in geographical coordinates, which can be referenced to the WGS84 datum used on charts and by mariners more generally.

The original area of coverage of the AMB data is for the whole of the Australian marine jurisdiction, which includes waters adjacent to the mainland, offshore islands and external territories. This dataset has been trimmed to the offshore eastern margin of Australia and reprojected for use within the Capel-Faust 3D model. Commands for loading data are listed in Appendix 1.

This dataset includes the following disclaimer:
AMB data is a digital representation of the territorial sea baseline and of the outer limits of Australia's maritime zones. The baseline and zones are established under the Seas and Submerged Lands Act 1973. The data also includes a representation of the limits by which the waters adjacent to each of the Australian States and of the Northern Territory are determined under the Coastal Waters (State Powers) Act 1980, Coastal Waters (Northern Territory Powers) Act 1980 and the Petroleum (Submerged Lands) Act 1967. In the event of an inconsistency between AMB data and the baselines and limits under the legislation, the latter prevails.

Data quality

Lineage:
The territorial sea baseline ('the baseline') data was originally derived from Geoscience Australia's 1:100 000 scale coastline data supplemented with coastal aerial photography in some areas. This mapping of the baseline was done in the early 1990's and since then the baseline data has been extensively validated and revised using the best available data from Geoscience Australia, the Australian Hydrographic Office and all State and Territory mapping agencies. The source material used for this purpose includes charts, topographic mapping, recent aerial photography and satellite imagery, as well as other miscellaneous sources, such as LADS data. Australia's baseline incorporates approximately four hundred straight baselines as proclaimed under the *Seas and Submerged Lands Act 1973*.

The location of the terminal points of these straight 1994 baselines were revised in 2005 to make them compatible with the Geocentric Datum of Australia (GDA94) as well as Geoscience Australia's most recent mapping of the baseline. These new locations have been incorporated into the baseline for AMB.

The various maritime limits that are derived as a distance from the baseline have been rigorously computed using specialised geodetic software rather than simple buffering. This software, known as MarZone was developed specifically for this purpose by the Department of Geomatics, University of Melbourne, under contract to Geoscience Australia.

Other maritime boundaries included in AMB have been digitised from their description in the relevant legal instrument such as treaty or legislation. Where necessary, these coordinates have undergone a datum transformation to be consistent with other AMB data.

Positional accuracy: The positional accuracy of the baseline varies according to the scale and origin of the source material, the data digitising process and the stability of the coastline. Experience and empirical evaluations suggest that the location of the baseline in AMB has been mapped to an accuracy generally better than 150 metres standard deviation.
As the maritime limits are rigorously computed no significant error is introduced in this process. Limits which are arcs, are represented by chords, with a one metre arc to chord tolerance. Boundaries digitised from a coordinate list, such as treaties, are as accurate as the stated coordinate and where applicable, the coordinate transformation method used. In general, the boundary data can be regarded as having been computed to an accuracy of one metre, whether it is derived from the baseline or a list of coordinates.

Attribute accuracy: Manual testing of the attribute items and values was performed on all of the data.

Logical Consistency: ArcInfo was used to do a topological consistency check to detect flaws in the spatial data structure and to flag them as errors. This check ensures that all classified polygons are closed, nodes are formed at the intersection of lines and that there is only one label within each polygon, etc.

Completeness: The AMB data contains a complete picture of Australia's jurisdictional boundaries, as well as, the territorial sea baseline and/or treaty lines from which they are derived.

3.2.2 Australian Coastline
GEODATA TOPO 250K Series 3

GEODATA TOPO 250K Series 3 (Geoscience Australia, 2006) is a vector representation of the major topographic features appearing on the 1:250 000 scale NATMAPs supplied in a shapefile format and is designed for use in a range of commercial GIS software. Data is arranged within specific themes. All data is based on the GDA94 coordinate system but was converted into WGS84 UTM57S for use in GOCAD™ and trimmed to show the east coast of Australia only.

GEODATA TOPO 250K Series 3 is also available as a packaged product in Personal Geodatabase or MapInfo TAB file formats. Each package includes data arranged in ten main themes - cartography, elevation, framework, habitation, hydrography, infrastructure, terrain, transport, utility and vegetation. Data is also available as GEODATA TOPO 250K Series 3 for Google Earth in .kml format for use on Google Earth TM Mapping Service. These datasets are available from Geoscience Australia (www.ga.gov.au; http://www.ga.gov.au/meta/ANZCW0703008969.html) under “Free Data Downloads”.

3.3 BATHYMETRY

Bathymetry data was acquired as part of the GA-2436 RV *Tangaroa* survey (2007), covering the NW corner of the Capel-Faust study area. The data was acquired using a Simrad Em300, a 30–34 kHz multi-beam sonar system, which was successful in obtaining good resolution data. The raw data was processed using CARIS HIPS/SIPS V5.4 software, removing noise and artefacts from the data and producing a 30 m and coarser 100 m grid of the area (Heap et al., 2009). These files were subsequently imported into ER Mapper, where processes such as sun shading were applied to enhance the grids appearance. The data was then exported as ASCII grids, as well as a high resolution GeoTIFF of the area. Given the dataset sizes, a 90 m resolution grid was used for the Capel-Faust region. In the LHR_Capel_Faust_3D_Time project, the GeoTIFF was loaded into the project and draped onto the seafloor horizon surface, providing high resolution information about the seafloor (Figure 4, commands listed in Appendix 1). In the LHR_Capel_Faust_3D_Depth project, the generated bathymetry surface built in the time domain was converted into depth using the processes outlined in Section 4.4.

A regional bathymetry dataset was compiled at horizontal resolution of 0.01° (~1 km) from the available swath bathymetry data, merged with trackline data, to create the national bathymetry grid by Webster and Petkovic (2005).

Swath bathymetry data are included from the following surveys by GA identifier: 222, 1152, 2312, 2357, 2359, 2411, 2418, 2436. These data were sub-sampled using Generic Mapping Tools (GMT; Wessel and Smith, 1991) program 'blockmedian' to achieve the desired input resolution for gridding and a total of 3 million data points. Levelled trackline data were included from the following surveys by GA identifier: 12, 52, 1151, 1504, 1560, 1584, 1589, 1592, 1670, 1892, 2411, and unlevelled data from GA survey 302, altogether another 188 000 points. Satellite-derived bathymetry data were not included which is sometimes done to fill gaps in the ship track coverage. The source datasets for the Capel-Faust regional bathymetry grid cover an area between the latitudes 25°–30°S and the longitudes 159°–164°E.

The data were gridded using the Intrepid software. Minimum curvature gridding with tension set at 0.5 was used and a regional grid at 1 km and coarser resolutions was produced. Because of issues with dataset size, a 2 km grid resolution was used within the 3D models. Both a time and depth version of the dataset was loaded into the GOCAD™ projects.

3.4 WELLS

The Capel and Faust basins are an exploration frontier, with all drilling on the Lord Howe Rise limited to the Deep Sea Drilling program (DSDP) and the Ocean Drilling Program (ODP). DSDP hole 208 is the deepest stratigraphic control in the Capel-Faust region. The hole intersected 594 m of recent to Maastrichtian sediment (Burns et al., 1973; Andrews, 1973; Figure 2). Well data and logs were downloaded from the National Geophysical Data Centre (NGDC) website (http://www.ngdc.noaa.gov/mgg/geology/dsdp/data/21/208/index.htm). These files were edited and converted from depth to time using velocities calculated in Petkovic (2010). The age markers and density and sonic logs were loaded into GOCAD™ using the commands listed in Figure 5 and Appendix 1. A location file PointsSet for DSDP holes was also loaded from an ArcGIS shapefile (Appendix 1). ODP 588 was located on the same site and drilled to a total depth of 246 m. Neither wells fully penetrate the post-rift succession of the Capel and Faust Basins. The syn-rift and pre-rift sediments of these basins currently remains undrilled.

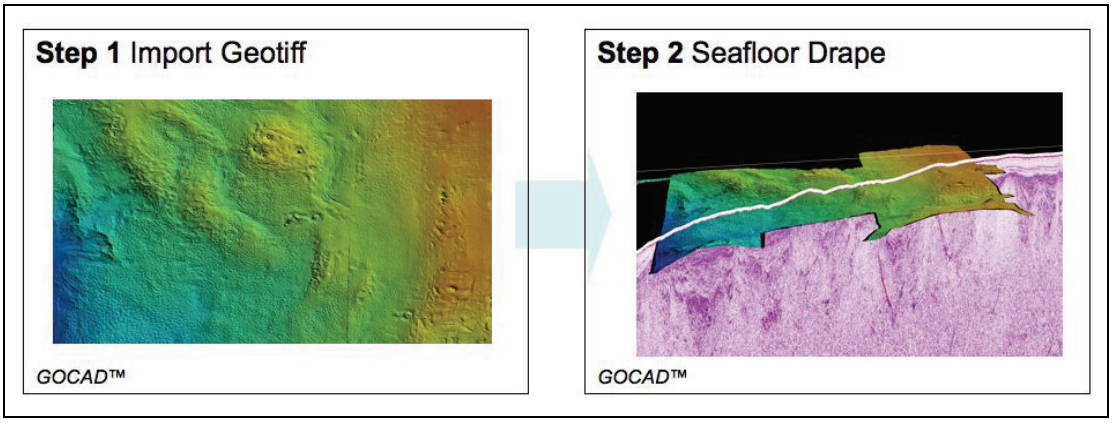

Figure 4: *Bathymetry data loading workflow.*

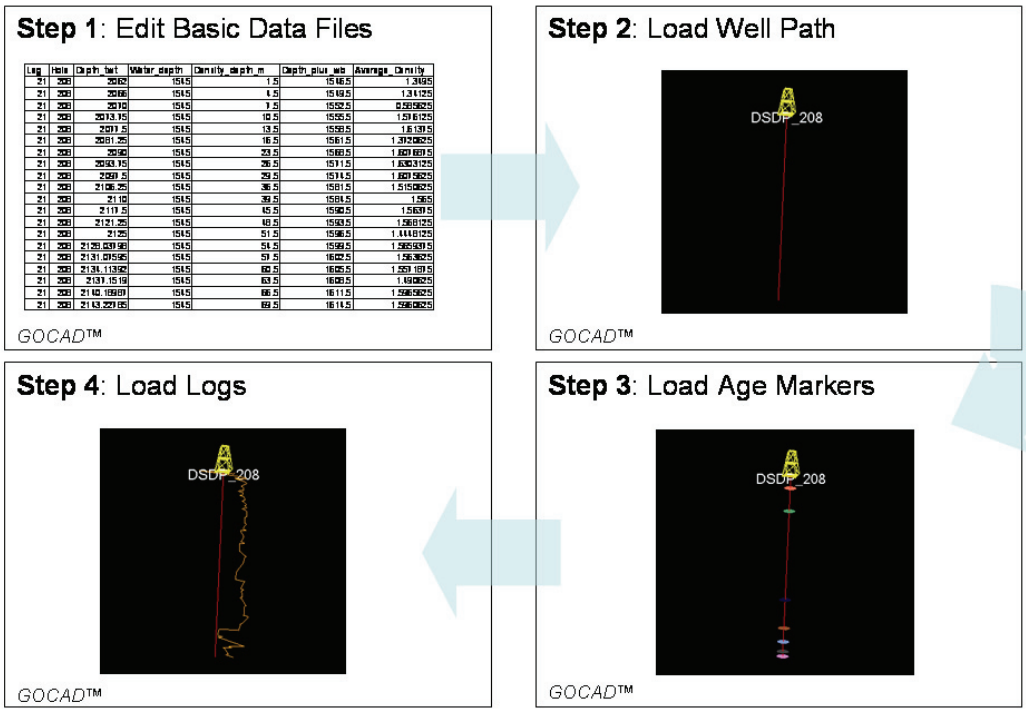

Figure 5: *Well data loading workflow.*

3.5 SEISMIC DATA

The Capel-Faust region is covered by two major reflection seismic surveys: GA-206 (also known as FAUST 1) and GA-302 (Figure 6).

The GA-206 2D seismic survey is a regional dataset acquired by Geoscience Australia on the RV *Rig Seismic* in 1998 to infill some of the pre-existing regional seismic grids on the Lord Howe Rise. Three reprocessed lines lie within the Capel-Faust region and were interpreted as part of the study (GA-206r/04 and 206r/02a and b; Colwell et al., 2010). The survey also recorded gravity and magnetic data.

The GA-302 2D seismic survey was acquired by Geoscience Australia in 2006–2007, focusing on acquisition within the Capel-Faust region. Data relationships between satellite gravity and the pre-existing GA-206 seismic survey lead to the GA-302 line placement being largely determined by filtered satellite altimeter-derived gravity data. Specifically, the survey targeted large gravity lows, which were previously observed to coincide with the location of large depocentres. The MV *Pacific Titan* acquired 23 lines of seismic, covering approximately 6000 line km. This provides good coverage of the Capel-Faust area with line spacing varying between 20–50 km. Magnetic and gravity data were also acquired.

Seismic SEGY was imported into GOCAD™ line by line as voxet files (commands listed in Figure 7 and Appendix 1). The water column and deeper sections of the seismic (where data quality was poor) were removed. Due to the high quality of the seismic and high data density, the resolution of the voxet files was also reduced. Finally, using the seafloor surface built in GOCAD™, the remaining water column in the voxets was made transparent.

Further information on seismic acquisition and processing parameters can be accessed in Colwell et al. (2010) and Kroh et al. (2007). Colwell et al. (2010) also contains digital images of interpreted and uninterpreted seismic sections. Seismic SEGY data is available from Geoscience Australia at the cost of transfer (contact: ausgeodata@ga.gov.au).

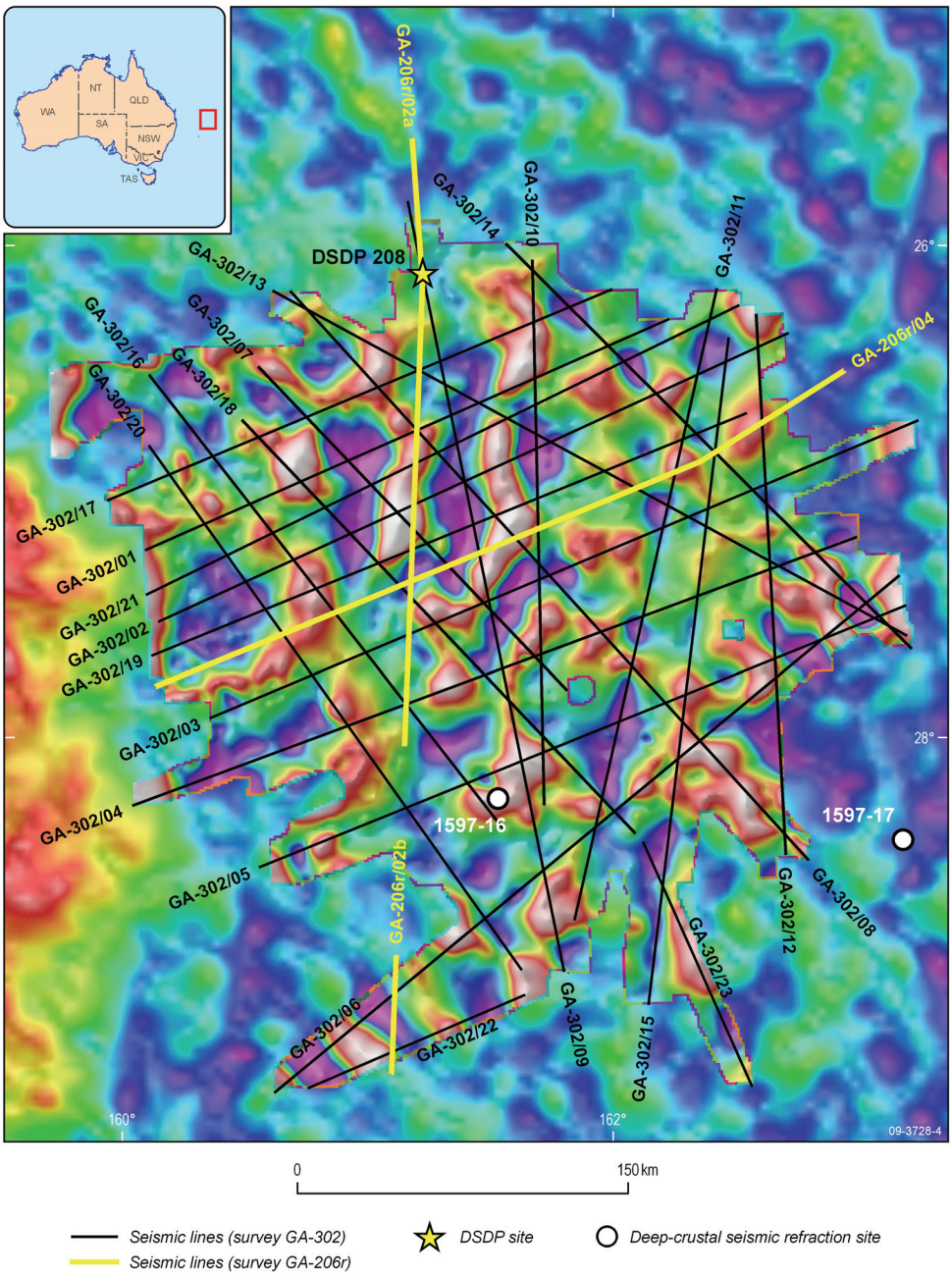

Figure 6: *Location of GA-206 and GA-302 seismic surveys. The background is an image of bandpass-filtered Bouguer gravity compiled from shipboard gravity superimposed on satellite altimeter-derived gravity beyond shiptrack coverage. Locations of previous deep-crustal seismic refraction experiments (1597-16 and 1597-17; Shor et al., 1971) are shown by the white filled circles.*

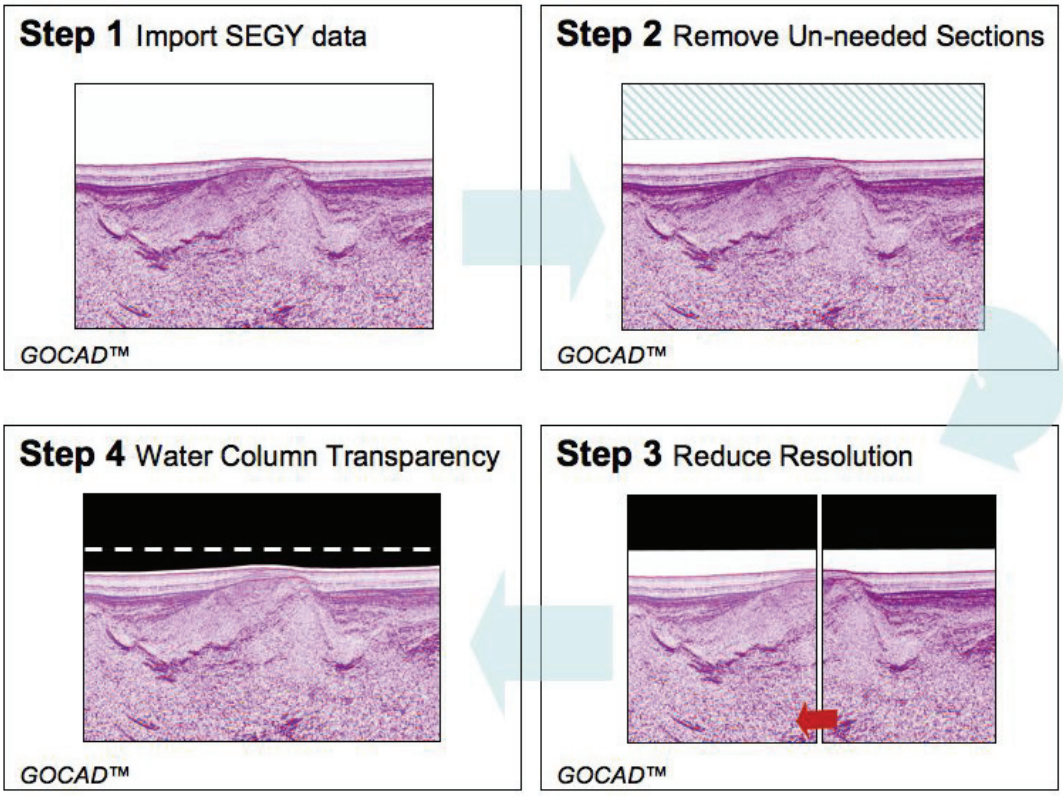

Figure 7: *Seismic data loading workflow.*

3.6 POTENTIAL FIELD DATA

The gridded potential field data included in the GOCAD™ project are based on data collected during the GA-302 and GA-2436 surveys (Figure 6). Magnetic data from earlier surveys are also included. The GA-302 and GA-2436 datasets were processed by Fugro Robertson Inc LCT Gravity and Magnetics Division (Fugro Robertson) and provided to Geoscience Australia in 2008. The preparation of gravity and magnetic datasets is summarised below. More details and information on improved and expanded datasets can be found in Hackney (2010).

3.6.1 Gravity Data

The line-based free-air gravity data were separately levelled by Fugro Robertson to minimise misties at ship-track cross-overs and line-filtered to smooth the profile data. The line data for each survey were then gridded separately using a 0.01º grid cell size and merged using the gridMerge tool within the Intrepid™ software. The merged free-air grid was then converted to Bouguer anomalies using a 0.01º grid of the bathymetry dataset described by Webster and Petkovic (2005). Terrain corrections were not applied.

The images included in the GOCAD™ project are band-pass filtered in order to enhance anomalies associated with upper-crustal structure. The low-pass cut-off is at a wavelength of 100 km (to remove long-wavelength components, most likely related to the Moho, and the high-pass cut-off is at a wavelength of 7.5 km; Figure 8a).

3.6.2 Magnetic Data

Fugro Robertson's initial processing of the line-based magnetic data involved correction for diurnal variations, levelling and line filtering. Anomalies were computed by subtracting appropriate versions of the International Geomagnetic Reference Field. The line data were separately gridded using a cell-size of 0.01º. The resulting grids were merged, not only with each other, but also with grids derived from data obtained during a number of additional surveys (Hackney, 2010).

The combined grid was reduced-to-pole in order to remove the dipole nature of magnetic anomalies and shift the anomalies to lie directly over their source. The reduced-to-pole data were low-pass filtered with a cut-off at 15 km wavelength (Figure 8b).

3.6.3 Multi-scale Edge Detection

Given the apparent correlation between gravity lows and depocentres evident in seismic reflection data (cf. Chapter 6), the multi-scale edge-detection method (Archibald et al., 1999; Hornby et al., 1999; Milligan et al., 2003) was used to aid the interpretation of structural linkages between seismic lines and to analyse dominant structural trends.

Major subsurface structures that coincide with significant density and susceptibility contrasts, such as fault offsets that juxtapose different rocks types, result in steep gradients in gravity and magnetic data. These gradients can be emphasised by computing the total horizontal derivative of the data, a measure of the gradient of the gridded data. The multi-scale edge-detection method automates the process of detecting horizontal gradient maxima and thereby aids in the detection of significant subsurface structures. The utility of the maxima points resulting from multi-scale edge detection is enhanced if they are converted into lines (also known as "strings" or "worms").

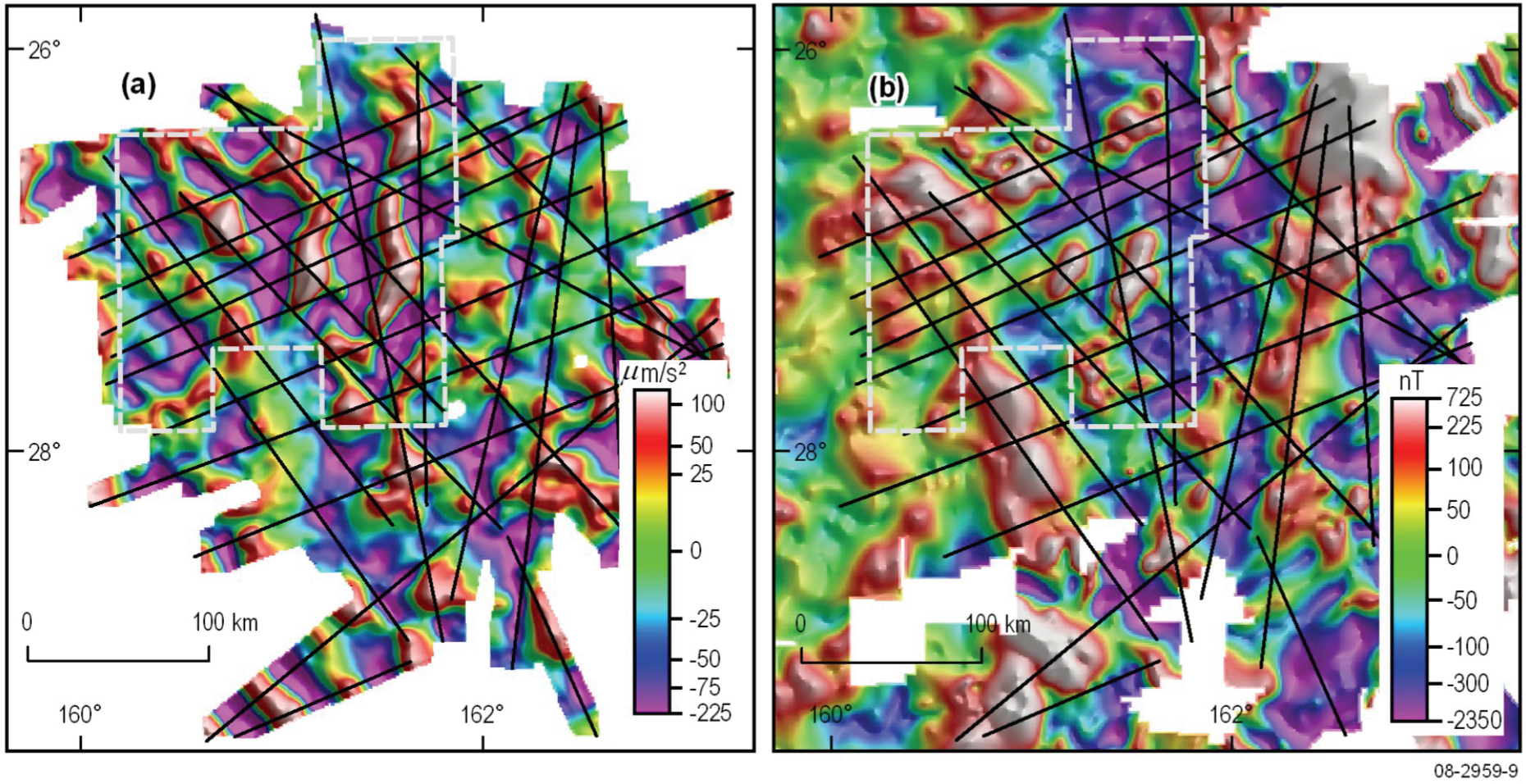

Figure 8: *Maps showing (a) band-pass filtered Bouguer anomalies and (b) low-pass filtered, reduced-to-pole magnetic anomalies. Black lines show the survey GA-302 ship-tracks along which data were measured and the grey dashed line outlines the GA-2436 survey area. Note that the true anomaly range is not preserved in the GOCAD™ projects because the grids have been shifted and scaled to conveniently position them with the seismic data.*

The method is multi-scale in that the horizontal gradient maxima are computed for various levels of upward continuation. Upward continuation smoothes the gravity or magnetic data and attenuates the shorter-wavelength components of the data related to shallow density or susceptibility variations. This means that when the edge-detection is applied to data upward continued to various levels, the gravity or magnetic signature of structures at various depths can be inferred.

In the area of the Capel and Faust basins, major faults have been interpreted from 2D seismic reflection data (Section 4.2, Figure 14). Inferring the continuation of these structures out of the plane of the seismic lines is aided by the areal coverage of the gravity and magnetic data (Section 4.2). Edge strings computed for the gravity and magnetic data (upward continued to various levels) can then be assigned to structures evident in seismic data and the off-line extension of the structures can then be inferred by tracing the edge strings between lines. Assuming that the trends of the resulting strings represent fundamental geological lineaments, such as fault sets, then those having high linearity may be selected and subjected to statistical directional analysis. Directions of linear data are usually displayed using circular histograms or "rose" diagrams, which were used extensively for structural analysis of the region (see Section 5).

Representative examples of multi-scale edge data generated for the Capel-Faust gravity and magnetic datasets are shown in Figures 9 and 10. The levels of upward continuation applied to the data are shown in Table 1. The lowest and highest continuation levels are determined by the cell size of the gridded data and the smallest horizontal extent of the area under consideration, while the intermediate levels are determined using a height multiplier of ~1.5.

Table 1: *Levels of upward continuation applied to gravity and magnetic data for multi-scale edge detection analysis. In the GOCAD™ projects these numbers have been simplified.*

LEVELS OF UPWARD CONTINUATION FOR GRAVITY DATA (METRES)	LEVELS OF UPWARD CONTINUATION FOR MAGNETIC DATA (METRES)
1351, 1756, 2283, 2968, 3858, 5015, 6520, 8476, 11019, 14325, 18623, 24210	1351, 1756, 2283, 2968, 3858, 5015, 6520, 8476, 11019, 14325, 18623

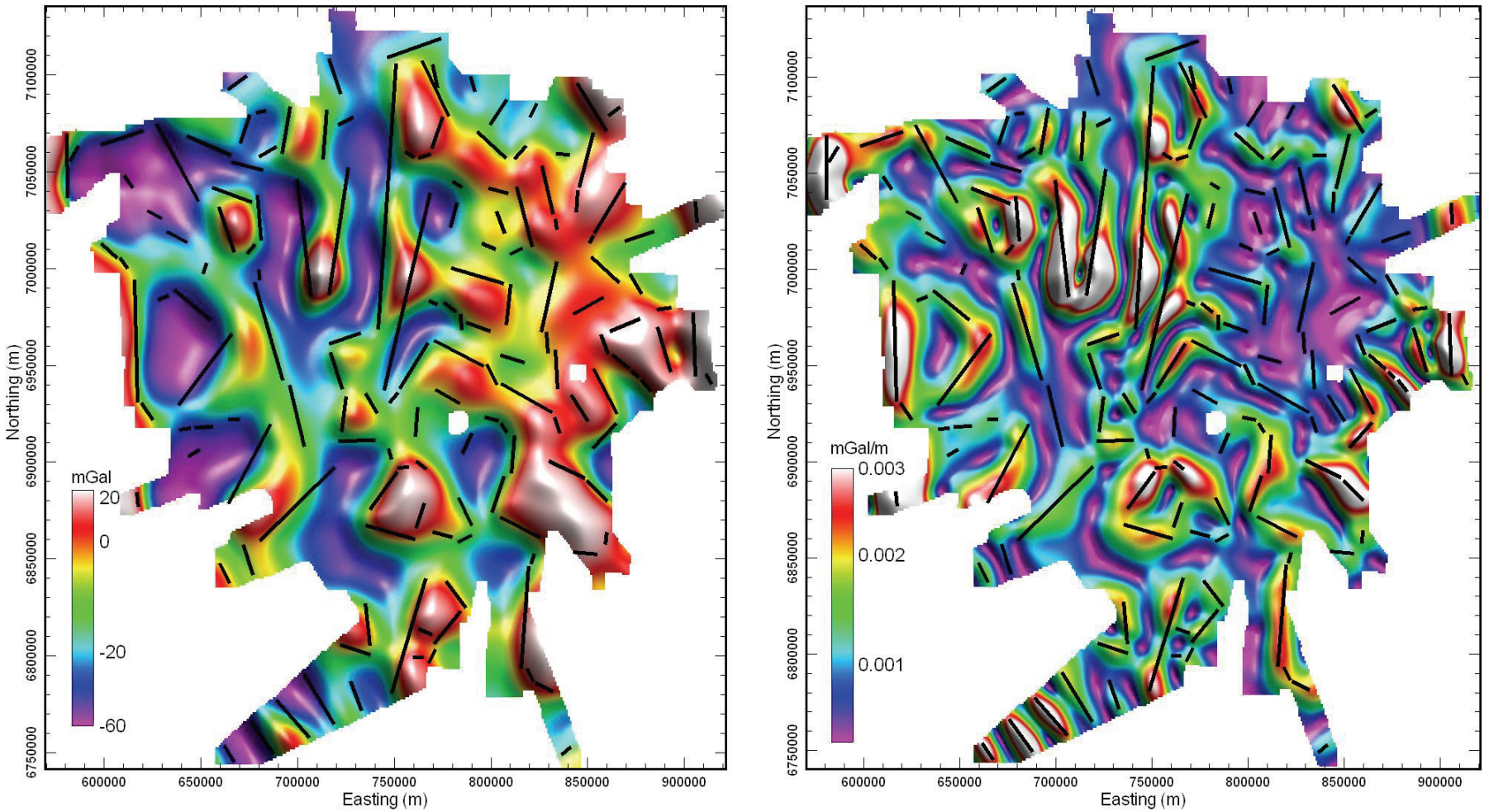

***Figure 9**: Maps showing gravity data upward-continued by 11019 m (left) and the total horizontal derivative of the data (right). Each image is overlain by straight line segments that represent the best fit to the most elongate total horizontal derivative maxima.*

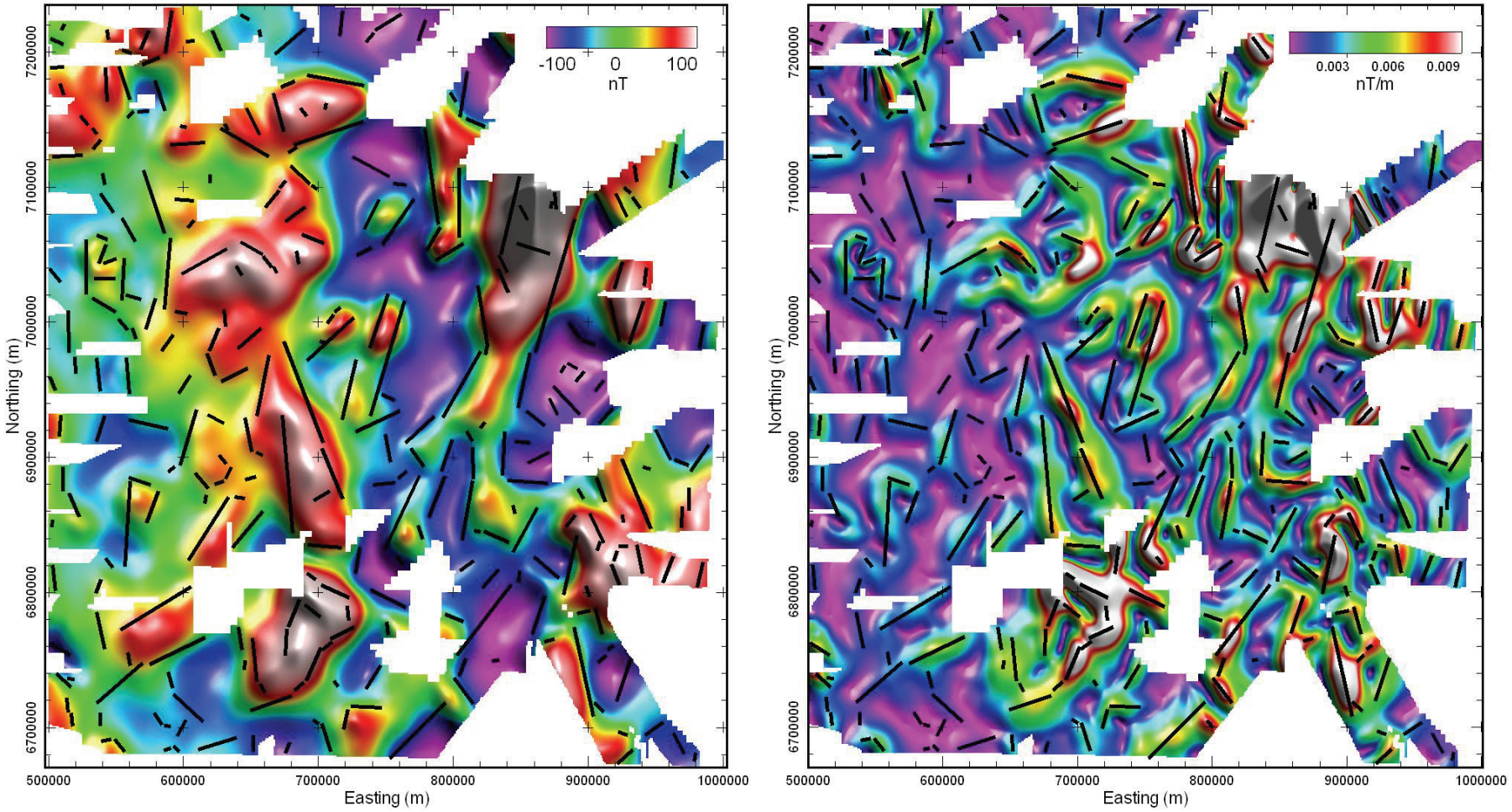

Figure 10: *Maps showing reduced-to-pole magnetic data upward-continued by 11019 m (left) and the total horizontal derivative of the data (right). Each image is overlain by straight line segments that represent the best fit to the most elongate total horizontal derivative maxima.*

4. Interpretation and Model Building

4.1 HORIZONS

Seismic horizon interpretation of the Capel-Faust region was undertaken on the GA-302 and GA-206 seismic surveys using the Schlumberger GeoFrame™ software. This data was exported in an ASCII format and imported into GOCAD™ as a series of PointsSet files (commands listed in Appendix 1). The horizon datasets are also available as a digital seismic interpretation project in GeoFrame™, Kingdom™ and Landmark™ workstation formats, as well as in GOCAD™ and basic ASCII formats.

A total of twelve seismic horizons were identified, relating to major unconformities. Age control for these horizons is only available from the seafloor to the Maastrichtian (DSDP hole 208; Section 3.4). Due to a lack of deep well control, age assignment for most of the horizons is tentatively linked to major regional tectonic events (Figures 11 and 12). More detailed information about the seismic horizons, the interpretation process and data downloads is available in Colwell et al. (2010).

Of the twelve horizons, seven were interpreted as being key horizons which would be incorporated in a 3D model (Figures 11 and 12). “Horizon7_ Top_Pre-rift” encompasses three different basement types (CF_Bmtv, CF_Bmtl, CF_Bmtb; Colwell et al., 2010) with variation between an interpreted “volcanic”, “layered” and a “bland” pre-rift basement. “Horizon6_Top_Synrift_1” is a major erosional surface associated with structuring and inversion at some localities. This unconformity has been identified regionally as a Cenomanian event, including along southern margin of Australia (Krassay et al., 2004) where there is well control. The underlying Syn-rift 1 megasequence represents the first major rifting event in the area, likely in the Early Cretaceous. “Horizon5_Top_Synrift_2” generally represents an erosional unconformity, marking the end of a second major rifting event in the area. At some locations the underlying Syn-rift 2 megasequence exhibits a sag, rather than syn-rift, stratal geometry. Major faults commonly terminate at this level. The remaining horizons are associated with post-rift sag deposition with minor structuring disrupting the stratigraphy. “Horizon4_Top_Lower_Sag” represents the deepest horizon with well control, occurring just below the Late Maastrichtian TD for DSDP 208. The horizon marks the separation of an upper and lower sag sedimentary unit. “Horizon3_Palaeocene-Eocene” and “Horizon2_Eocene-Oligocene” represent regional unconformities. “Horizon1_Seafloor” represents the seafloor.

These horizons were interpreted with picks continuing up major structures and over the top of basement highs. Grids from these horizons form a “blanket” model across the region rather than a true “geological” model, which would have horizons terminating against basements highs and faults. This was done so that a completed horizon surface from this interpretation could be viewed independently in 2D software environments. By having a continuous surface rather than a segmented surface, a velocity model could be built using the horizon grids as intervals for depth conversion (see Section 4.4). The continuous surface could also be used for geohistory modelling (see Section 4.5). Once a “blanket” model was complete a second version was created from these horizons that represent a true “geological” model. These horizons are not regionally extensive, pinching out on the edges of depocentres, as well as terminating on faults. See Section 4.3 for further information about this process.

The horizon interpretation was loaded into the GOCAD™ and Petrosys environments (Figure 13). Initial grids of the horizons were created within Petrosys using its “Grid, contour, volumetrics” capabilities. Key parameters and commands are listed in Appendix 1. A 5 km grid spacing was used due to a minimum seismic line spacing of approximately 20 km.

The resulting grids were loaded into the GOCAD™ as 2D-Grids and refined using a number of processes (commands listed in Appendix 1). Firstly the 2D-Grids were converted into a horizon surface. The interpretation points loaded from GeoFrame™ into GOCAD™ were then assigned as

control points on to the appropriate horizon surfaces. Horizon surface editing then proceeded. Each gridded surface had the resolution optimised to best match the interpretation points. This approach was decided upon rather than having a gridded surface set to a particular cell size, determined by an appropriate level of scale, and unable to match all interpretation points. The end result of this process was smaller cells next to, and on, the seismic line controls and larger cells further away from the seismic lines. This allows the gridded surface to accurately match its interpretation control where it is present. This helped to capture the structural and stratigraphic complexity of the region. Each surface was also decimated, another process for influencing the surface resolution, that uses aspect as a controlling factor. Steep slopes require smaller cells to accurately depict them, where as planar areas need less, larger triangles for accurate representation. Each horizon surface was then "beautified", a GOCAD™ specific term referring to the removal poorly shaped triangles. Finally minor adjustments to the surfaces was completed by moving individual nodes, setting extra controls on the surface, splitting triangles within certain areas and interpolating the surface, or regions therein, to take into account these changes. Once an acceptable 3D horizon surface was created, a series of isopach maps were generated including major unit thickness isopachs (such as Syn-rift 1, Syn-rift 2 etc.) and a total sediment thickness from the top of pre-rift basement to the water bottom. The unit thicknesses were used to set range thickness constraints on individual horizon surfaces, influencing any further interpolations during surface refinement.

The final horizon surface outputs were used to create a velocity model for the region (Section 4.4), fed into the geohistory modelling workflow (Section 4.5) and used for the final model integration of horizons and faults (Section 4.3).

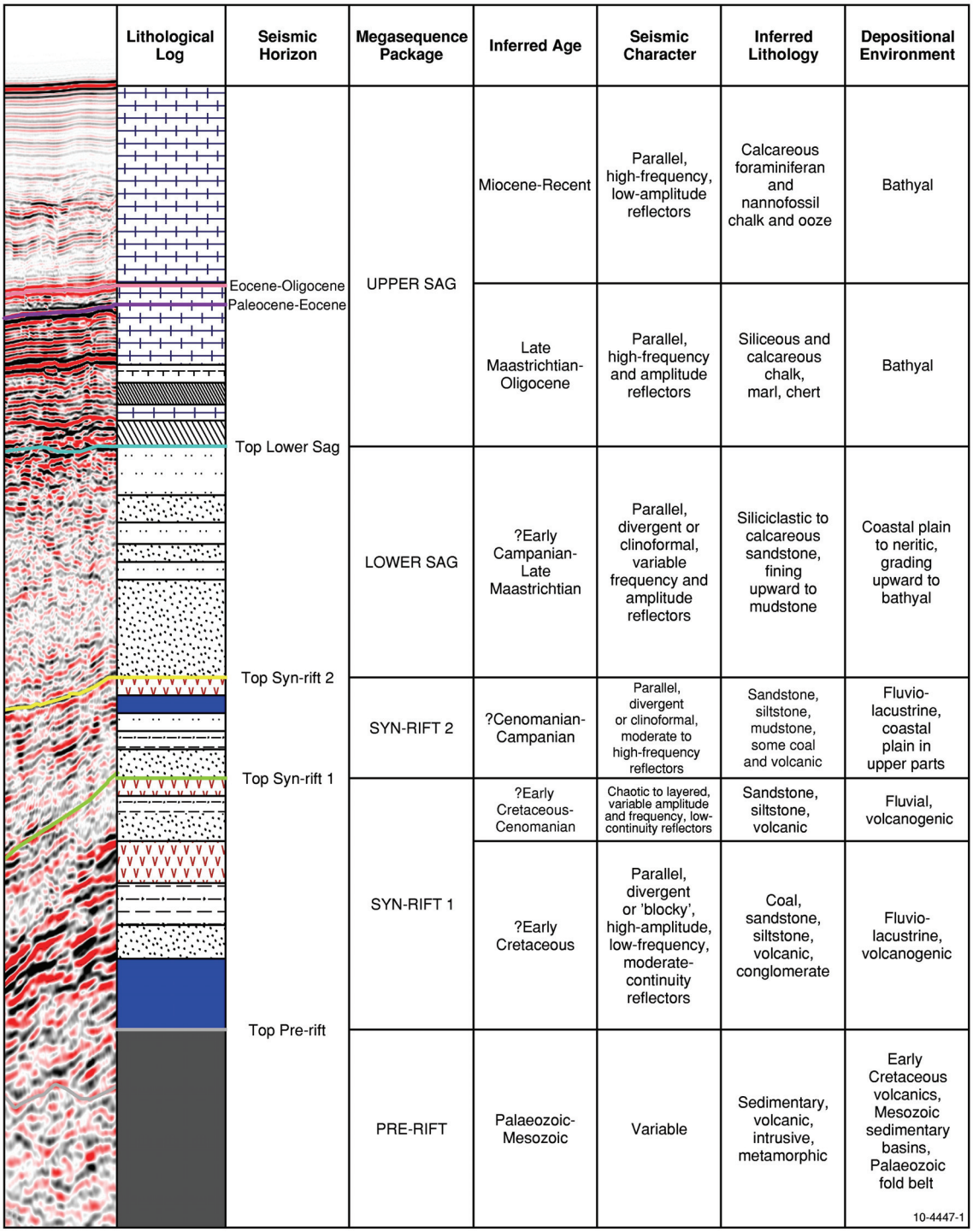

Figure 11: *Geological interpretation of seismic megasequences for the Capel-Faust region.*

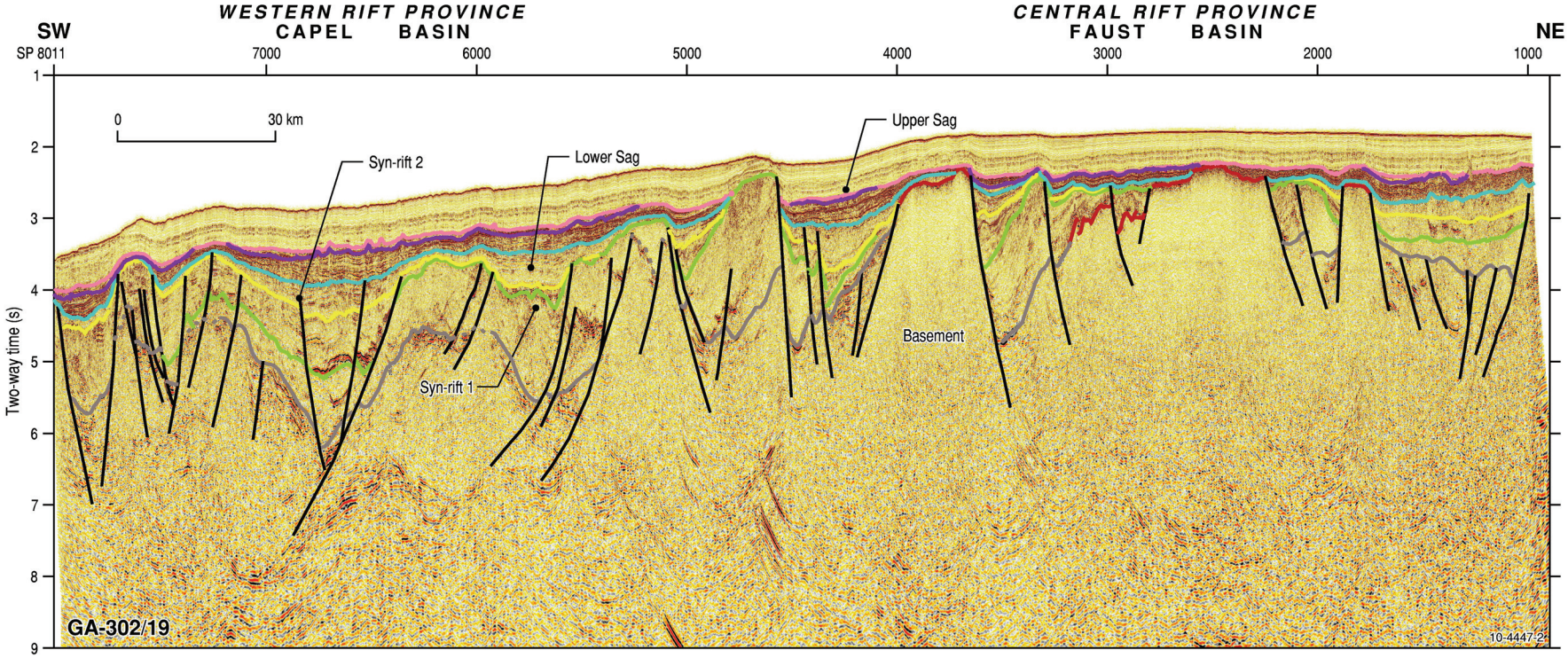

Figure 12: *Seismic line GA-302/19 showing the general rift architecture of the northern Lord Howe Rise across the Capel and Faust basins. Location of the seismic line is shown in Figure 2 (after Colwell et al., 2010).*

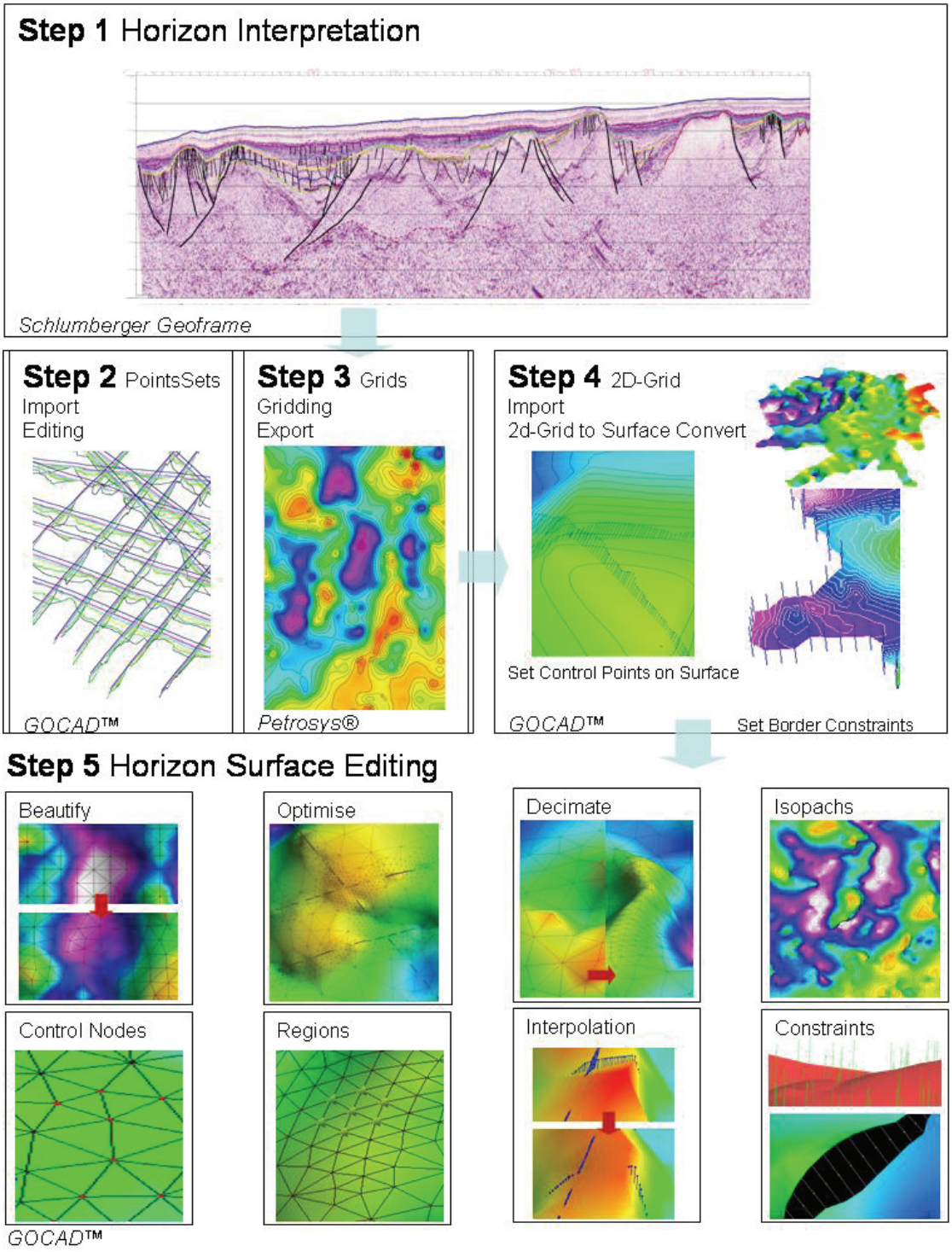

Figure 13: *Horizon surfaces workflow.*

4.2 FAULTS

Seismic fault interpretation of the Capel-Faust region was undertaken on the GA-302 and GA-206 data using the Schlumberger GeoFrame™ software. The interpretations were exported in an ASCII format and imported to GOCAD™ as curve files (commands listed in Appendix 1). The fault datasets are also available as a digital seismic interpretation project in GeoFrame™, Kingdom™ and Landmark™ workstation formats, as well as in GOCAD™ and basic ASCII formats.

Two fault types were interpreted in the seismic datasets; a major basin-bounding or basement offsetting fault set ("Major_Faults") and a minor intra-basin fault set ("Minor_Faults"; Figure 14). More detailed information about the faults, the interpretation process and data downloads is available in Colwell et al. (2010). Both fault sets were imported into GOCAD™, with the expectation that the major fault set curves could be joined at some locations to form 3D fault surfaces (Figure 15). The minor fault set was also loaded to give a sense of fault style and kinematics within the depocentres.

Trends and relationships in the seismic, potential field and bathymetry datasets were used to constrain the structural model (Figure 15). An interpretive set of curves defines identified trends in the bathymetry and potential field data. The potential field data was also processed to produce worm datasets (Section 3.6) and simplified orientations which highlight large gradient and trend changes within these datasets. It should be noted that not all the trends in these datasets will relate to structures. For example, in the seismic data, it is clear that a number of steep gradients seen in the gravity data relate to sedimentary pinch-outs over basement ramps rather than faults. The fault surfaces ("Fault_Surfaces") reflect a compilation of the interpreted structure trends identified in these datasets.

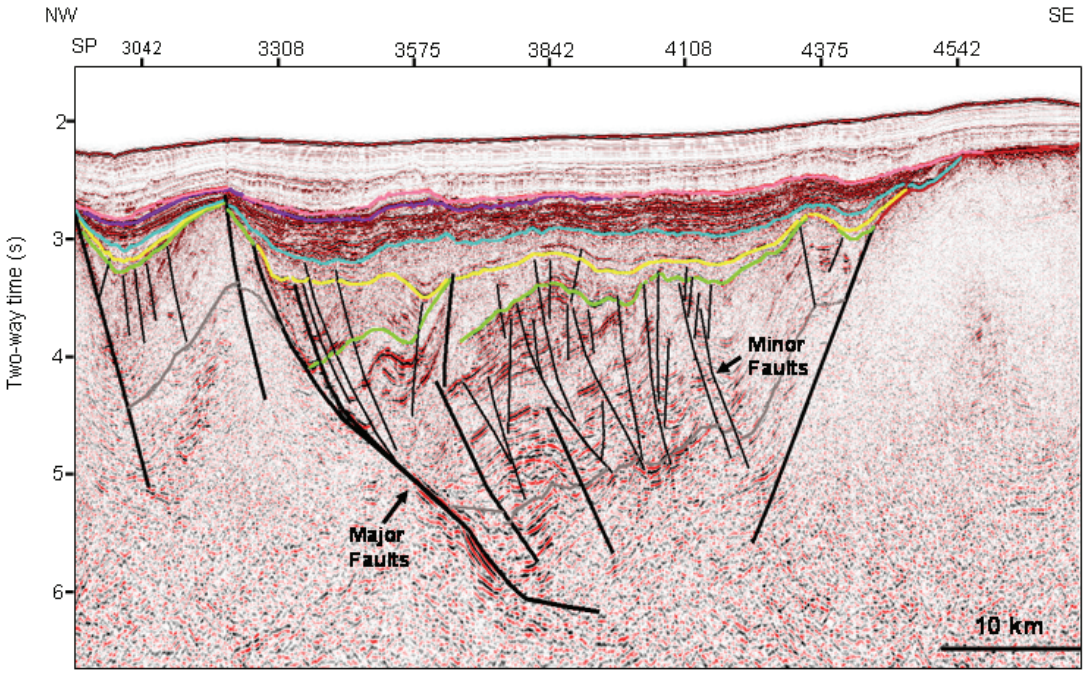

Figure 14: *Seismic image with major and minor fault set. Refer to Figure 11 for horizon names and ages.*

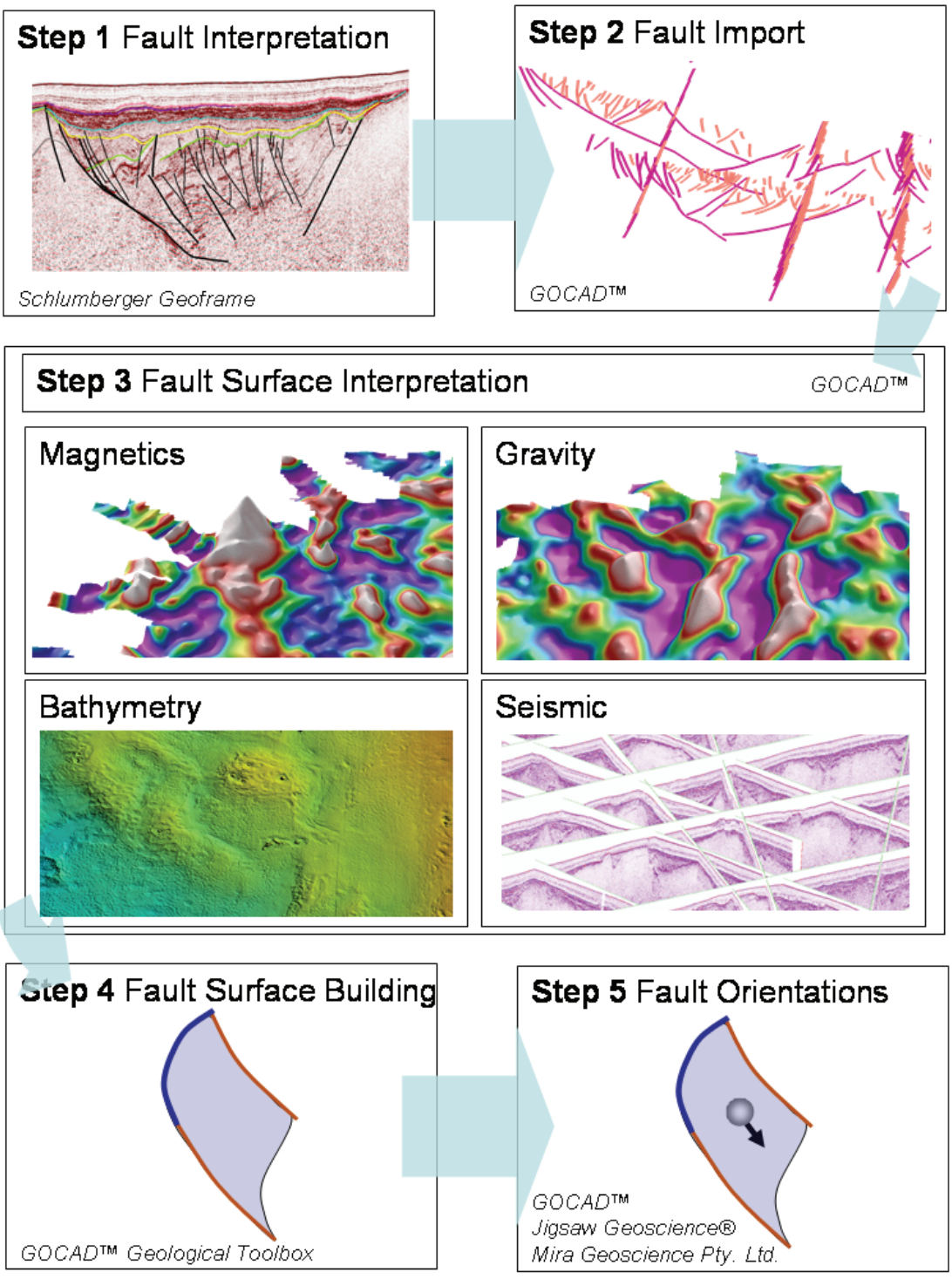

Figure 15: *Fault surface generation workflow.*

The fault surfaces were built by creating a curve map ("Fault_Curves") defining how the seismic fault cross-section curves join to form surfaces. The fault curve map was also extended off section beyond the seismic control, defined or interpreted from other datasets such as potential field data. Some faults were built using no seismic interpretation control but where other data suggested the presence of a fault.

Once a final fault curve map was completed fault surfaces were built involving both the curve fault map ("Fault_Curves") and the seismic fault cross-section curves ("Major_Faults") using the Geological Toolbox "Fault Builder" plugin (available from the GOCAD™ Consortium, http://gocad.ensg.inpl-nancy.fr/www/consortium/index.xhtml). Where no seismic cross-section curves were present to control fault height and dip, a geological interpretation of other datasets in the area was used to produce reasonable constraints.

Orientation data was generated for the final fault surfaces using a script and a wizard provided collaboratively by both Jigsaw Geoscience and Mira Geoscience. This process produced a PointsSet ("Fault_Orientation_Data") where orientation is captured as a vector property encapsulating the fault orientation, dip and dip direction. This allowed the generation of fault stereonet plots from the PointsSet using a "Stereonet" plugin (available from the GOCAD™ Consortium, http://gocad.ensg.inpl-nancy.fr/www/consortium/index.xhtml). These plots highlight what the dominant interpreted faults trends are, for comparison with other datasets where orientation data is available. A "dip_direction" property was also added manually to the fault surfaces file to capture gross changes in east and west dipping faults to assist with accommodation zone interpretation.

The final fault surface outputs were fed into the geohistory modelling workflow (Section 4.5) and used for the final model integration of horizons and faults (Section 4.3).

4.3 HORIZON-FAULT INTEGRATION

Horizon-fault integration refers to the final stages of 3D model construction. Up to this point horizon and fault surfaces are independent objects, allowing for greater flexibility in regards to interpretation editing and adjustment. Once the objects have been finalised, the horizon and fault surfaces can be integrated together, capturing tectonostratigraphic relationships.

The commands used for this process are listed in Figure 16 and in Appendix 1. Due to the extent of the study area and the number of fault surfaces coupled with the main area of interest for prospectivity being limited to the NW and central regions, where the basins are deepest and biggest, it was decided to only integrate horizons and faults in these areas. The end result of this process are a series of horizon surfaces "cut" by fault surfaces, highlighting structural style and growth during sedimentary deposition. The visualisation of the structural movement was enhanced by creating surfaces that represent fault displacement, connecting fault tops and bottoms for each horizon (shown in the 3D model as curve files). The total fault displacement for each horizon surface was computed in GOCAD™ and painted onto the fault displacement surfaces (Figure 16). This growth generally shows the maximum fault displacement occurring in the middle of the fault and pinching out towards the edges, as expected. Where multiple faults have joined to form one long fault, surface fault growth and pinch-out patterns show where the smaller original fault segments are likely to occur. This process adds insight into the regions development history and produces a complete, fully integrated 3D model.

Once this process was completed on the "blanket" 3D model, the finalised horizons were duplicated and edited to create a "geological" 3D model. This involved further editing, removing large sections of the surfaces on features such as basement highs, creating pinch-outs and drapes. The final output is two models, "blanket" and "geological", which serve different purposes. The "blanket" model allows examination of a single horizon, particularly useful in 2D software packages, whereas the "geological" model uses all horizons to gain a complete, more accurate geological picture.

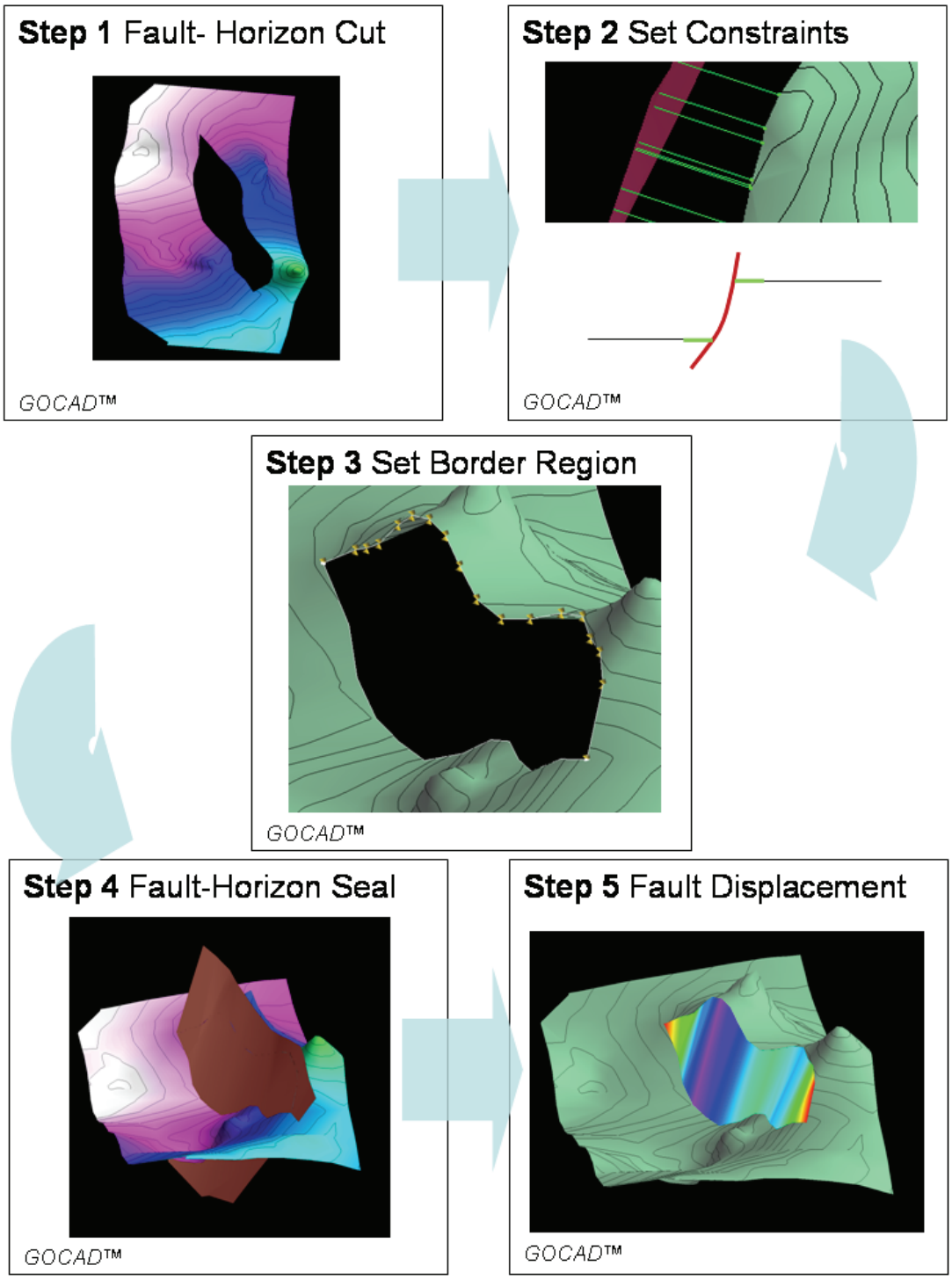

Figure 16: *Fault horizon integration workflow.*

4.4 DEPTH CONVERSION

The initial seismic interpretation and the constructed 3D model lie within the time domain. To convert the datasets, their associated interpretation and the final 3D model into depth a velocity model of the region is needed. GOCAD™ has the capabilities to build a "Velocity Model Voxet" encompassing all datasets, using either interval velocities, a continuous function, or a combination of both.

In the Capel Faust region, velocities can be calculated from sonobuoy refraction results or interval velocities derived from stacking velocities (Petkovic, 2010). As no deep wells are present in the region there are no velocities available from well data, although a comparison between shallow depth converted results can be made with DSDP hole 208. Three velocity models were created for the region; one each from the stacking and sonobuoy data represented as continuous quadratic velocity functions with origin at the water bottom, and one using calculated interval velocities for the interpreted geological horizons.

The interval velocity model was built by assigning key horizon surfaces as geological features, enabling them to be used to define regions within the Velocity Model Voxet (commands listed in Figure 17 and Appendix 1). Once regions were defined, a new property was created called "velocity" and a script was applied to assign different velocities to different intervals within the voxet. This process was similar for both continuous functions downwards from the water bottom by implementing the algorithm so velocity increased down-section. The water body was given a fixed velocity of 1500 m/s. A new property was created capturing average velocity, which is calculated by a GOCAD™ function using the velocity property. This average velocity property removes sharp changes in velocity. Once a model was complete, with an average velocity, it can be used to convert any dataset within its area from time to depth.

The depth converted results for each velocity model were assessed and compared. The continuous functions produced the best depth conversion results. The stacking velocity function best matches results from DSDP 208 in the shallow section, but gives unrealistically high sediment velocity with increasing depth. The sonobuoy function produced a more realistic velocity at maximum sediment depth. The end result of these tests was to use a combination velocity model, using a fixed interval velocity for the water column, the stacking velocity derived function in the shallow subsurface and sonobuoy velocity function at depth.

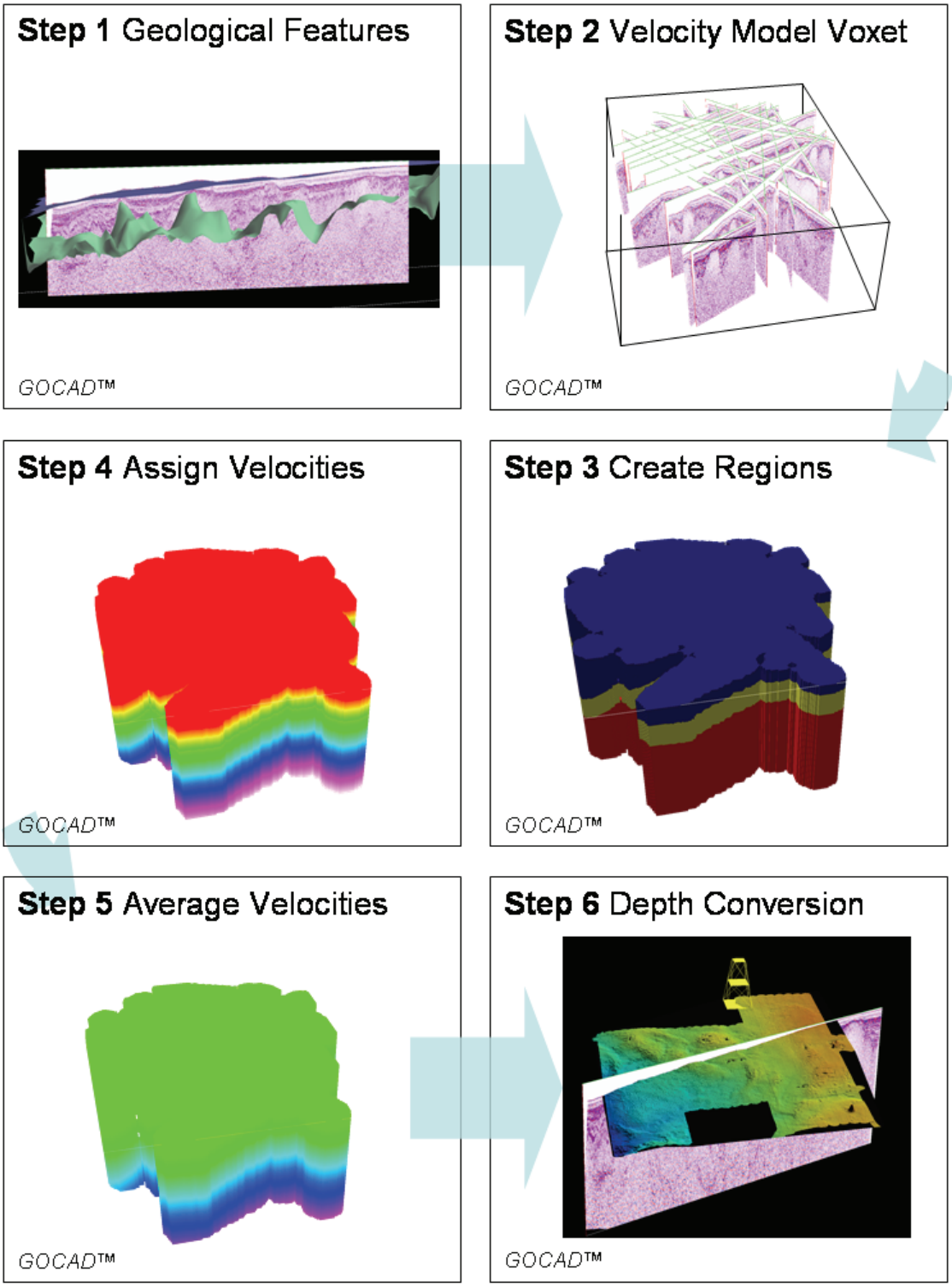

Figure 17: *Depth conversion workflow.*

4.5 INTEGRATION OF OTHER ANALYTICAL WORKFLOWS: EXAMPLE OF GEOHISTORY MODELLING

Multi-1D basin (geohistory) and charge modelling was carried out in the study area in collaboration with GNS Science (New Zealand) to predict the likely maturity of potential petroleum source rocks present in the study area and the location of hydrocarbon migration pathways and accumulations (Hashimoto et al., 2011). Although basin and charge modelling, per se, were carried out independently of the GOCAD™ environment using the BM1D code (GNS Science) and the Trinity software (ZetaWare Inc.), the work provides an illustration of the ease with which external workflows may potentially be integrated with the GOCAD™ workflow.

Seven gridded seismic horizon surfaces from "Horizon7_Top_Pre-rift" upward to "Horizon1_Seafloor" (Section 4.1), created and depth-converted in GOCAD™, were exported in ASCII format as inputs to the basin models. An additional surface depicting the maximum depth of pre-rift sediments (as identified on seismic data) was also used to constrain the base of the basin model. Progressive deposition, burial and heating of the basin succession were modelled at each cell within the area covered by the grids using: stratigraphic thickness and palaeo-bathymetry (a surrogate for palaeo-temperature) derived from the grids; age, lithology and source rock parameters inferred from regional correlations with eastern Australia and New Zealand, and; heatflow history based on present-day near-surface measurements, a simple two-phase (130–100 and 95–80 Ma) rifting model and elevated crustal heat flow due to post-rift magmatism (68–60 and 27–18 Ma; Funnell and Stagpoole, 2011).

Oil and gas generation were modelled using source rock kinetics of Pepper and Corvi (1995a, b), while migration and accumulation were predicted from the gridded seismic horizon surfaces assuming pure buoyancy-driven up-dip flow, with 3D major fault surfaces exported from the GOCAD™ model (Section 4.2) used as lateral baffles to migration.

The outputs of basin modelling at each cell within the area of grid coverage were aggregated to produce 2D map-based outputs for the entire area of coverage. These outputs were exported as shapefiles and ASCII grids and returned to the GOCAD™ environment as spatial layers to facilitate visualisation of relationships with the basin structure. These spatial layers depict total predicted expulsion volumes, per unit area, of oil and gas from the Pre-rift, Syn-rift 1 and Syn-rift 2 source rock intervals, and hydrocarbon migration pathways and accumulations at the stratigraphic levels "Horizon7_Top_Pre-rift", intra-Syn-rift 1, "Horizon6_Top_Synrift_1", intra-Syn-rift 2 and "Horizon5_Top_Synrift_2". For details on the results of basin modelling, readers are referred to Funnell and Stagpoole (2011).

As the base inputs to the basin models were derived from the GOCAD™ geological model, the basin modelling workflow has effectively been integrated as a subsidiary workflow loop to complement the GOCAD™ workflow in this study. The 3D environment of GOCAD™ has assisted in visualisation and interpretation of the results of basin modelling, which would otherwise have been restricted to a 2D map view.

5. Structure Analysis

The 3D structural model of the Capel-Faust region was built by coupling both interpreted trends in key datasets, such as seismic, gravity, magnetics and bathymetry, with processed potential field datasets, such as gravity and magnetic worms and their extracted trends (Sections 3.6 and 4.2). This produced a robust final fault model that has been built by effectively using all available scientific data.

The final structural model indicates that the architecture of the Capel-Faust basins is structurally complex, composed of a number of segmented depocentres. Faults are dominated by two main trends grossly aligned N–S and NW–SE (Figure 18). Processed gravity worms from potential field datasets also reflect these trends. Upward continued gravity data consistently show two dominant trends at all levels (1–24 km), one aligned along a NW–SE to NNW–SSE axis and another aligned along N–S to NNE–SSW axis trends (Figure 19). The N/NNE trend, however, is generally more dominant being the prevalent trend at all upward gravity continued levels. The two main trends also consistently exhibit the longest line lengths, as can be seen in the 3D model, with a maximum line length of 138 km for the N/NNE trend and 88 km for the NW/NNW trend, indicating more continuous, larger features. At upward continuation levels 4, 5 and 7 km a secondary NE–SW trend is evident, roughly orthogonal to the NNW/NW trend. Another secondary trend is apparent at levels 11 and 14 km, aligned NW–SE.

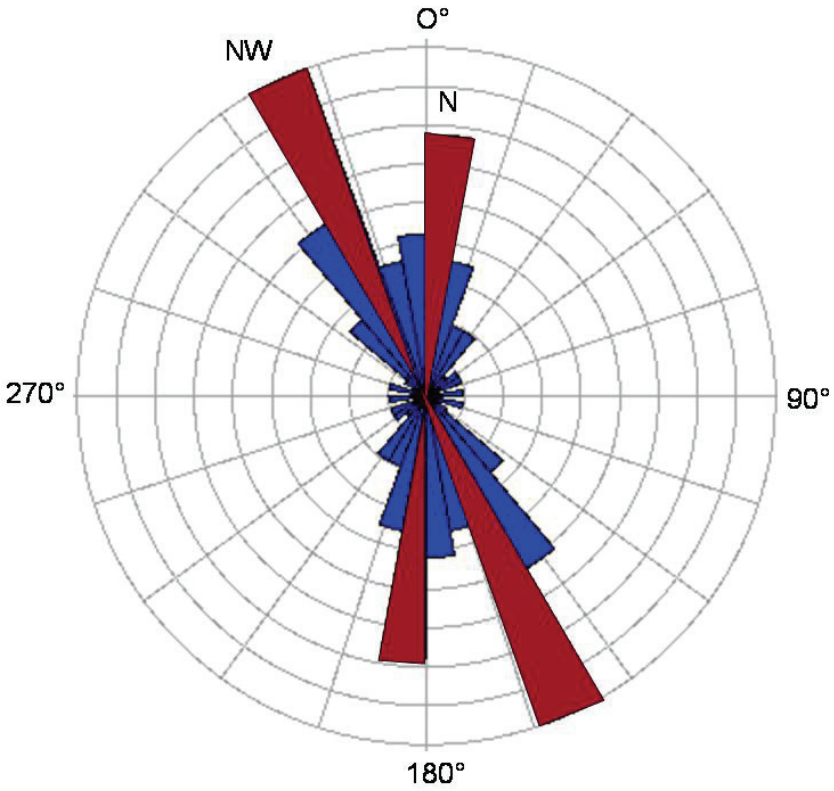

Figure 18: *Plan view rose diagram showing the strike of faults from the Capel-Faust geological model. Dominant trends are shown in red.*

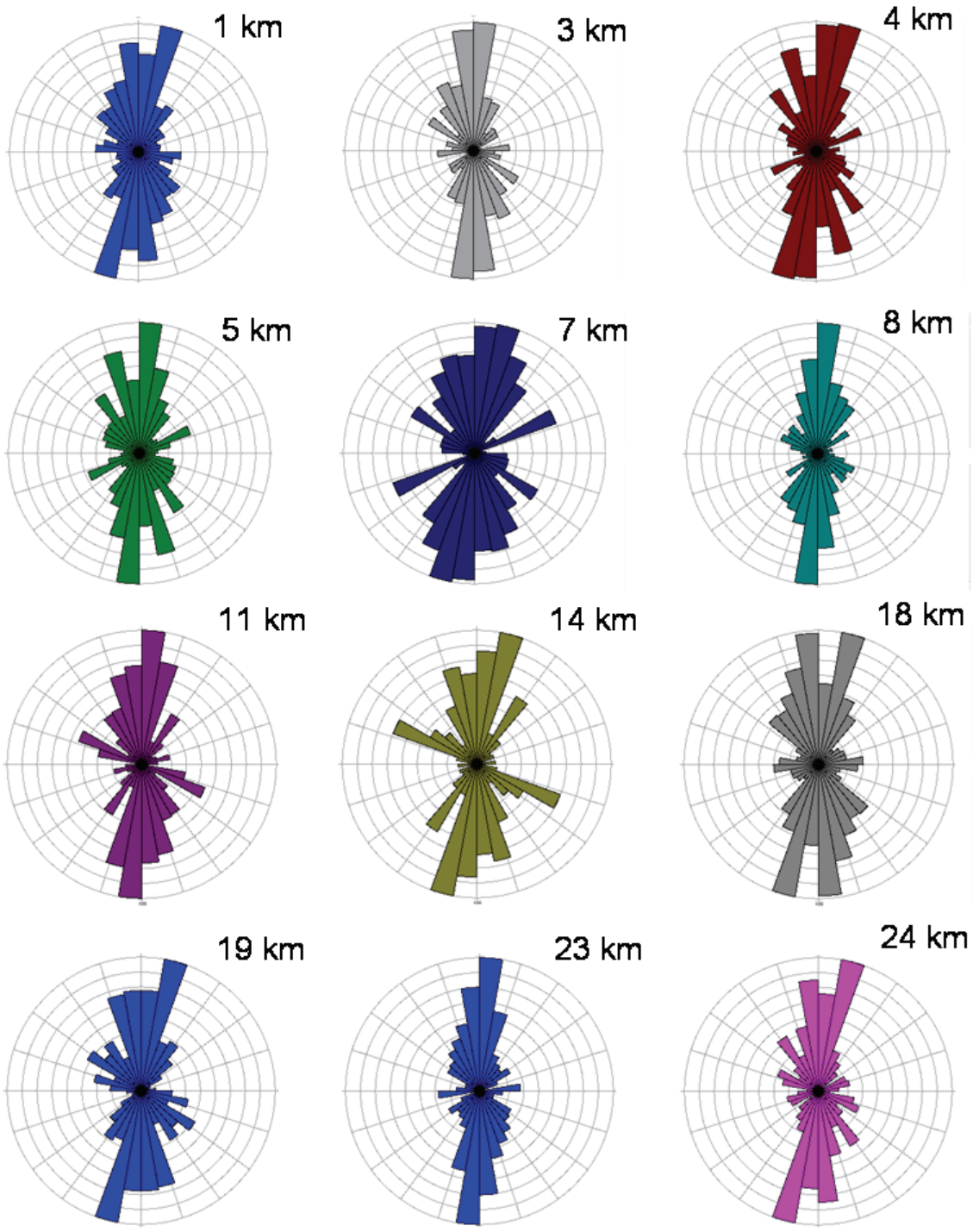

Figure 19: *Plan view rose diagrams showing gravity upward continuations of fault strike trends at levels 1–24 km.*

Trends apparent in the upward continued magnetic data are much more variable and segmented compared to those in the gravity data. The magnetic anomalies in the study area appear to be influenced to a degree by local variability in crustal composition, particularly the presence of igneous bodies such as dykes. As such, the derived trends do not entirely reflect the underlying architecture. However, the dominant trends observed in the magnetic data are aligned along NW–SE/NNW–SSE and N–S/NNE–SSW axes as with the gravity data (Figure 20).

The spatial distribution of the two dominant structural trends varies across the Capel and Faust basins. The major N-trending structures are restricted to the central region of the study area (Figure 21a), whereas the flanking areas to the west and east are dominated by NW-trending structures (Figure 21b). This structural zonation can be seen in both the gravity and magnetic datasets (Figure 21c and d); the central area is dominated by N-trending gravity highs and lows (Figure 21c) and is a magnetic low (Figure 21d), while the western and eastern areas are dominated by NW-trending gravity anomalies (Figure 21c) and is a magnetic high (Figure 21d). In both the gravity and magnetic data the boundaries between these structural zones follow a NW-trend and appear to be offset by NE-trending features in places (Figure 21c and 21d).

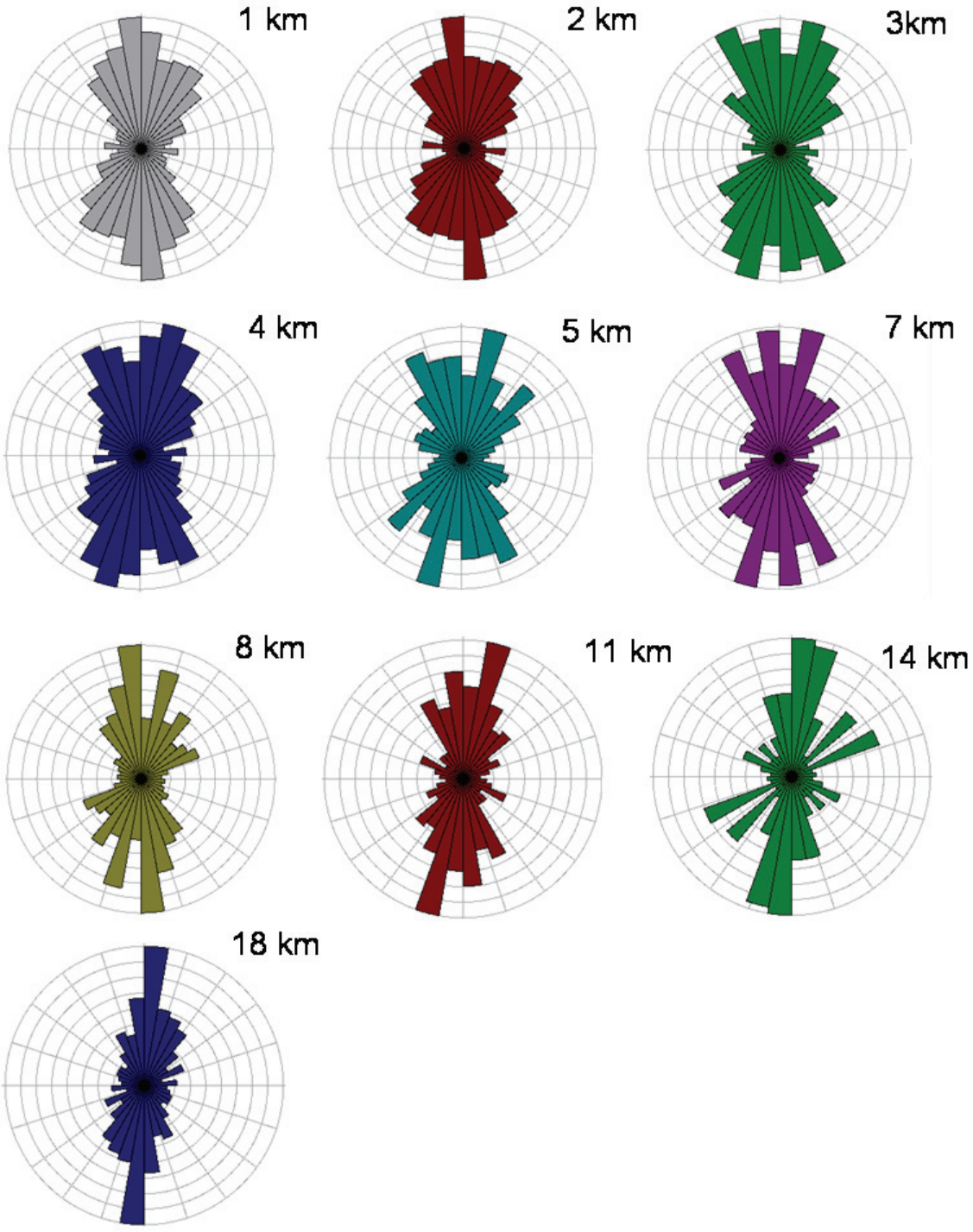

Figure 20: *Plan view rose diagrams showing magnetic upward continuations of fault strike trends at levels 1–18 km.*

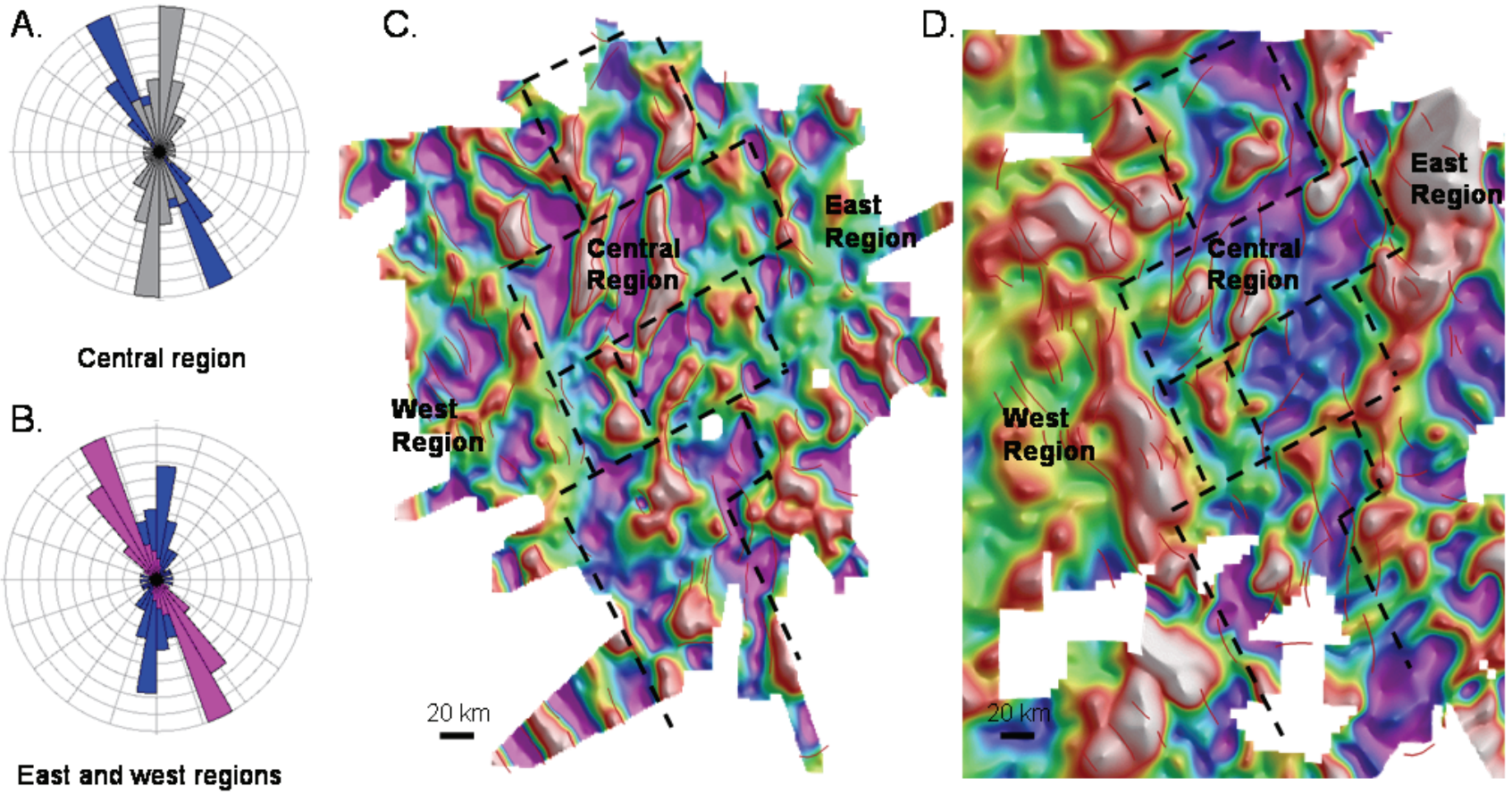

Figure 21: *(a) Rose diagram of the interpreted fault trends in the central structural domain showing dominant fault trends in grey. (b) Rose diagram of the interpreted fault trends in the eastern and western structural domains showing dominant fault trends in pink. (c) Bandpass-filtered Bouguer gravity with mapped major faults (shown in red) and interpreted changes in structural and depocentre trends (west, central and eastern regions). Black dashed lines represent interpreted NE-trending structural offsets in potential field data. (d) Magnetic data trends with mapped major faults (shown in red) and interpreted changes in structure and depocentre orientations (west, central and eastern regions). Black dashed lines represent interpreted NE-trending structural offsets in potential field data.*

6. Geological Interpretation

6.1 BASIN ARCHITECTURE

The Capel-Faust 3D model captures the complex architecture of the basins, composed of a number of graben and half-graben depocentres of variable extent. The Capel and Faust basins were originally defined by Stagg et al. (1999) and Willcox et al. (2001), who placed the boundary between the two basins at a large west-dipping fault seen on seismic lines from survey GA-206. Across this boundary, a change from the dominantly east-dipping faults of the Faust Basin to the dominantly west-dipping faults of the Capel Basin was observed (Figure 22). The original basin boundary was extrapolated away from the seismic lines based on regional satellite gravity and bathymetric data.

The 3D model clearly indicates that the area is structurally more complex than originally interpreted and that the previously defined boundary between the two basins does not reflect the subsea geological structure. The Capel and Faust basins are composed of a number of compartmentalised depocentres, rather than two broad basins. The central and northwestern area tends to contain the largest, deepest depocentres with dimensions of up to 150 km long and 40 km wide. These depocentres contain a maximum of 3.7 s TWT (~6.7 km) of sedimentary rocks (Figure 23b). The depocentres trend dominantly N–S in the central area and NW–SE in the northwestern area. The southern and eastern depocentres are significantly smaller and contain a thinner sedimentary succession but exhibit trends similar to the larger depocentres.

Analysis of structural trends indicate that there are two dominant N- and NNW-aligned fault trends in the Capel and Faust basins (Section 5; Figures 18, 19, 20 and 21) which are also reflected in the alignment of the depocentres (Figure 21 and 23a). The secondary NE–SW and NW–SE trends apparent in the upward continuations of gravity data appear to be derived from obliquely trending faults near the tips of main depocentre-bounding faults and areas that appear to have acted as accommodation, relay or transfer zones during faulting. These zones are defined by the roughly linear alignment of basement (gravity) highs separating neighbouring depocentres and the associated bounding fault terminations (Figure 21c). They also correspond to the NE-trending offsets in the magnetic anomalies (Figure 21d). The presence of these accommodation/relay/transfer zones have contributed to the compartmentalised architecture of the Capel and Faust basins.

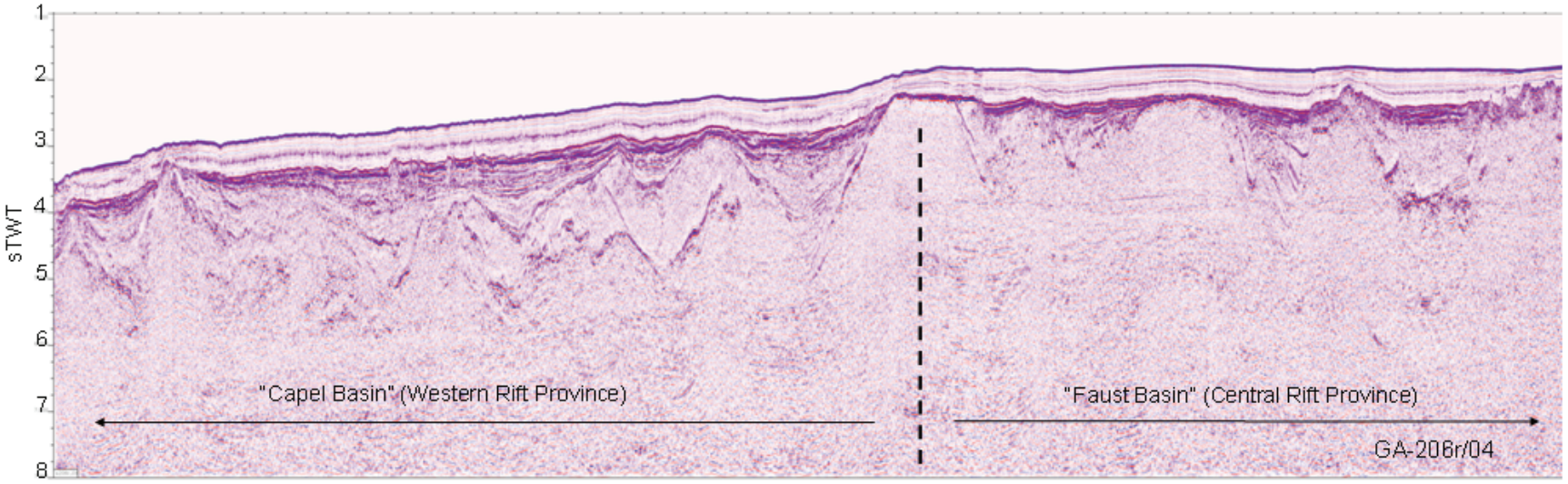

Figure 22: *Original boundary between the Capel and Faust basins as interpreted by Stagg et al. (1999) and Willcox et al. (2001) based on seismic line GA-206r/04.*

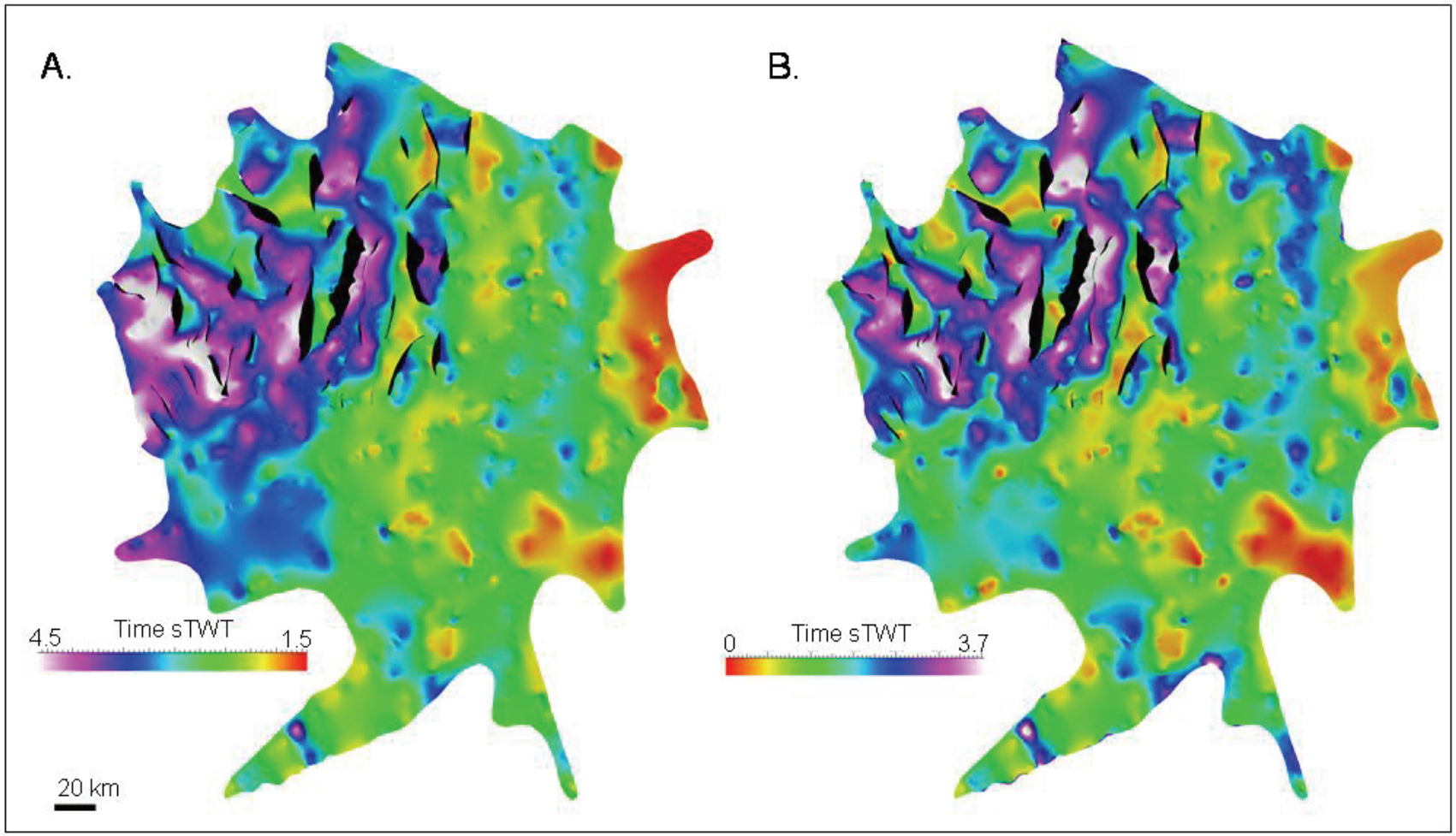

Figure 23: *(a) Structure of the Capel and Faust basins at the top pre-rift basement level. (b) Total sediment thickness from top pre-rift basement to the seafloor in the Capel and Faust basins.*

6.2 RIFT EVOLUTION

The rift depocentres in the Capel and Faust basins formed as part of the breakup of eastern Gondwana, which started in the Early Cretaceous and culminated in the opening of the Tasman Sea (c. 85–52 Ma; Gaina et al., 1998).

The interpretation of GA-302 seismic data has indicated that rifting in the Capel and Faust basins took place in two main phases, which were followed by post-rift thermal subsidence. Moreover, major structuring events have interrupted deposition during syn-rift and post-rift phases, resulting in local inversion, uplift, erosion and gentle folding (Colwell et al., 2010).

The first rifting event in the Capel and Faust basins, the Syn-rift 1 phase, is inferred to have begun in the Early Cretaceous (Colwell et al., 2010) and was focused in the central zone of the area (Figure 24a). As can be seen in the Syn-rift 1 isopach map (Figure 24a), N-trending depocentres were formed, within which up to 2.5 s TWT (~5 km) of sediment was deposited over the pre-rift basement. The first rifting event was terminated by a major inversion and erosion event, interpreted as the equivalent of the Cenomanian unconformity seen on the southern margin of Australia and coinciding with regional uplift in eastern Australia (Colwell, 2010; Norvick et al., 2001, 2008). In the Capel and Faust basins, there are a number of features related to this event. In the central and north-western depocentres, this includes reverse movement on major depocentre bounding faults, basin inversion and the formation of pop-up structures (Figure 25), which have contributed to extensive erosion. In the smaller depocentres in the south and east, the event is characterised by minor basin inversion.

The second rifting event, the Syn-rift 2 phase, is inferred to have taken place from the Cenomanian onward (Colwell et al., 2010). The locus of rifting appears to have migrated westward, as seen in the marked thickening of the Syn-rift 2 succession in the NW-corner of the study area (Figure 24b). Furthermore, rifting during this phase reactivated NW-trending faults in these depocentres. Up to 1.5 s TWT (2.8 km) of sediments were deposited over the Syn-rift 1 succession. The focusing of rifting to the westernmost areas, and its inferred timing, suggest that this episode represents crustal extension leading up to the opening of the Tasman Sea west of the Capel and Faust basins (Norvick et al., 2008; Colwell et al., 2010). Previous work indicates a general westward decrease in crustal thicknesses across the northern Lord Howe Rise (Shor et al., 1971; Zhu and Symonds, 1994; Willcox et al., 2001), indicating an increase in the degree of crustal extension towards the Tasman Sea Basin. Rifting was probably terminated due to the opening of the Middleton and Tasman Sea basins at this latitude during the Campanian–Maastrichtian (Gaina et al., 1998; Norvick et al., 2008). The NE-trending accommodation, relay and transfer zones align with the transform faults in the Tasman Sea Basin, and some offset of depocentres and basement highs is observed on these trends within the Capel and Faust basins (Figure 21c and d). This suggests that NE-trending strike-slip faulting may have affected the area during and after the Syn-rift 2 phase, as the Middleton and Tasman Sea basins opened to the west. Another major episode of structuring followed the Syn-rift 2 phase, causing erosion and gentle folding of the syn-rift successions (Colwell et al., 2010). This has created large anticlinal features, particularly in the north-western corner of the study area (Figure 25b).

Subsequent deposition after rift failure in the Capel-Faust area is characterised by a post-rift sag succession with up to 3.5 s TWT (~2.3 km) of siliciclastic to calcareous marine sediments, with sedimentation focused over pre-existing depocentres. In addition, Cenozoic volcanism is widespread throughout the region (Slater and Goodwin, 1973; McDougall et al., 1981; Exon et al., 2004; Colwell et al., 2010; Dadd et al., 2011; Higgins et al., 2011).

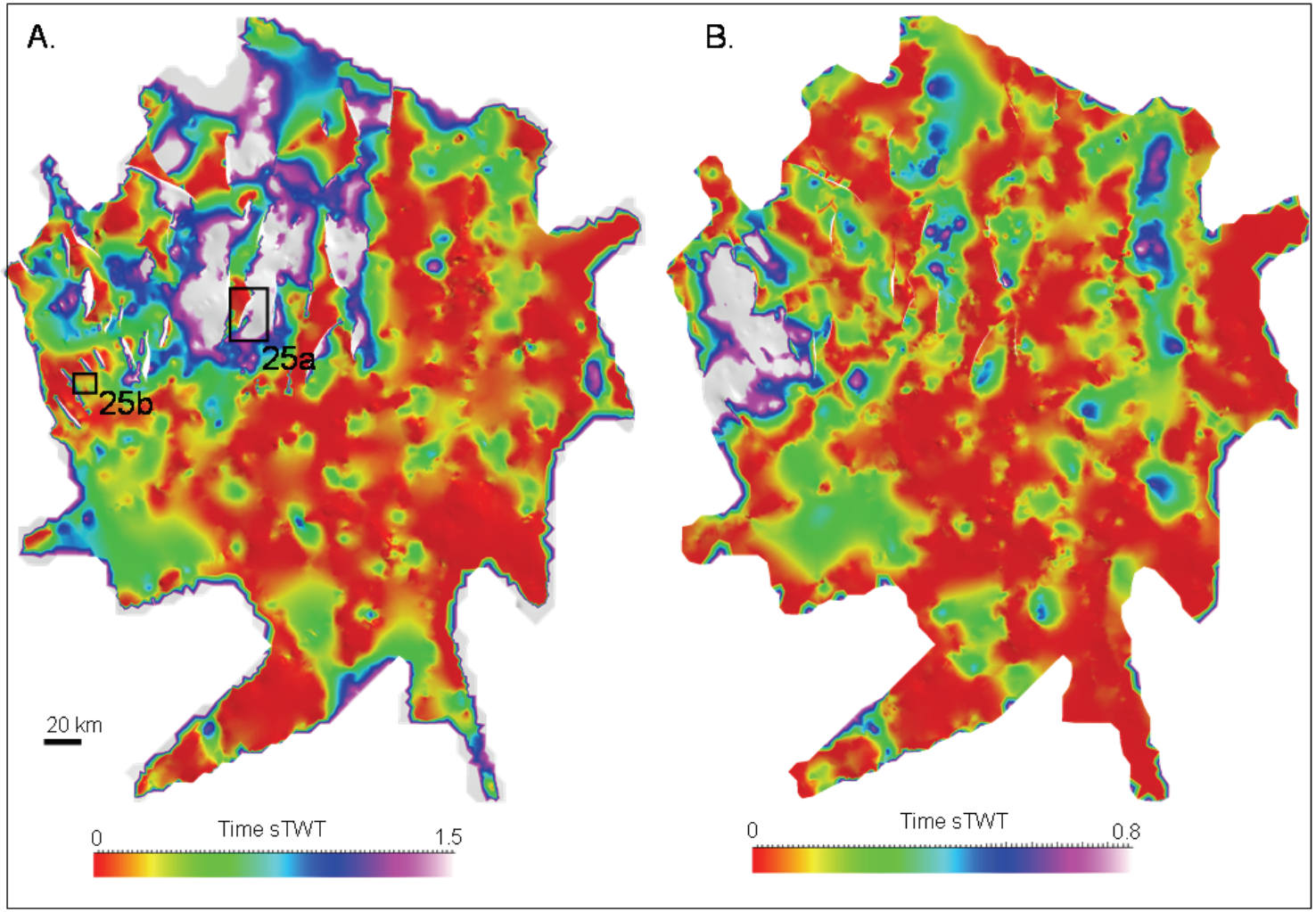

Figure 24: *(a) Total thickness of Syn-rift 1 megasequence. Locations for features in Figure 25 are also shown. (b) Total thickness of Synrift 2 megasequence.*

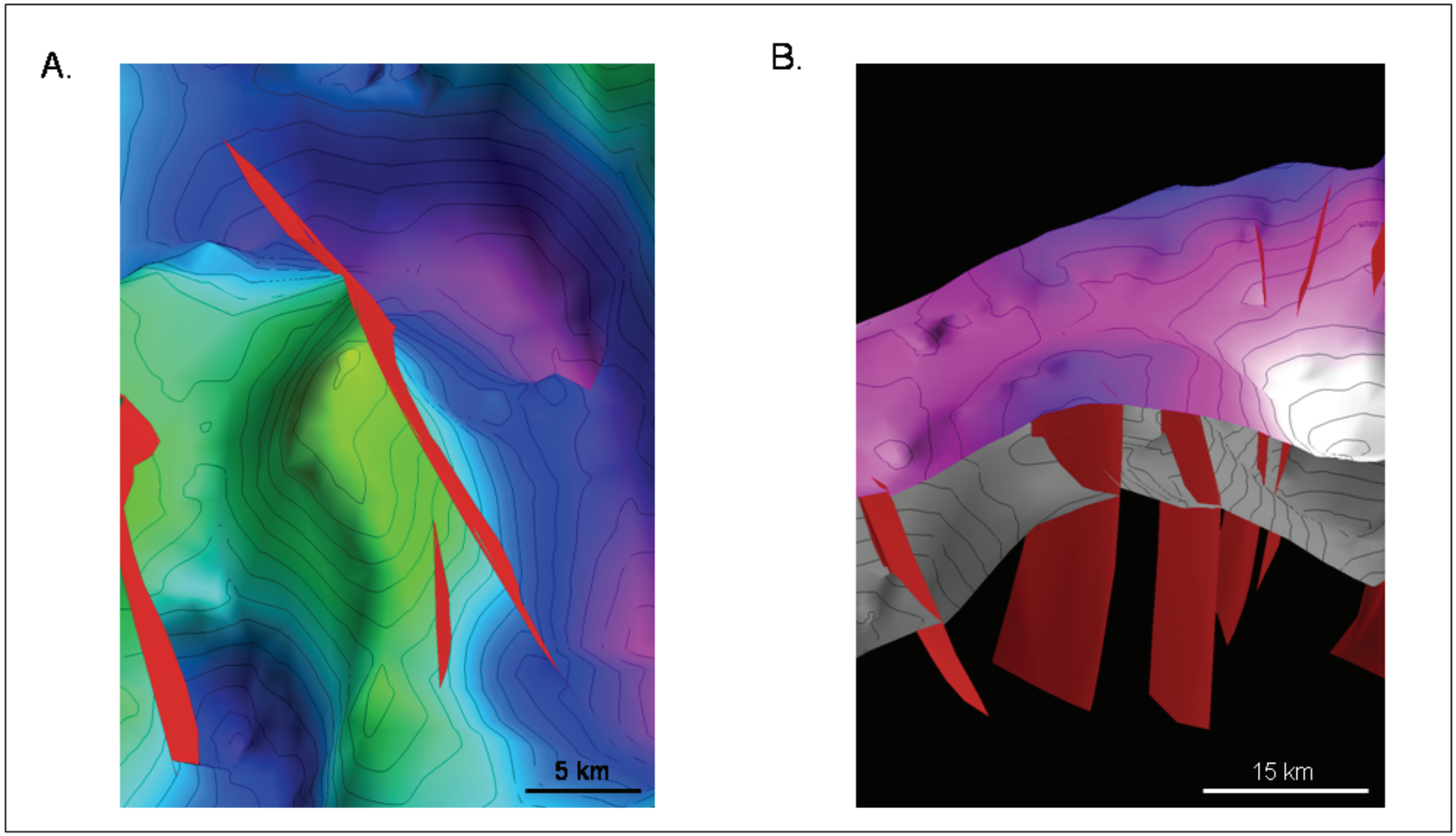

***Figure 25**: (a) Syn-rift 1 inversion anticline. (b) Syn-rift 2 anticline. Locations on Figure 24a.*

The structural zonation of the Capel and Faust basins into a central rift zone of N-trending faults and flanking zones dominated by NW-trending structures may be analogous to theoretical sandbox models of oblique rifting by McClay et al. (2001; Figure 26). McClay et al. (2001) show that if there is a pre-existing structural fabric oblique to the extension vector, the intra-rift faults will form orthogonal to the extension direction, while the rift border faults will be aligned with the original structural fabric. As such, the NW-trending structure within the Capel and Faust basins could be related to a pre-existing regional structural grain, while the central zone represents intra-rift depocentres and faults formed during the Syn-rift 1 phase. The angle of divergence between these trends would suggest a Syn-rift 1 extension vector oriented at 60° to a pre-existing trend NW-trend, approximately E–W. The highly segmented, en echelon to sigmoidal form of the faults agrees with this model (McClay et al., 2001). The NE-trending accommodation, relay or transfer zones (Figure 21) would therefore have formed during this rifting phase. Faults in the western zone of the Capel and Faust basins were subsequently modified by further rifting during the Syn-rift 2 phase. The reactivation of the NW-trending Syn-rift 2 faults probably reflects a shift in the extension vector to a more northeasterly direction, arising from the northward-propagating transtensional regime of the Tasman Sea rifting (Gaina et al., 1998; Norvick et al., 2008). Cross-sections for the McClay et al. (2001) model (Figure 26b) display a similar architecture to seismic cross-sections through the Capel-Faust region (Figure 26d), although the Capel-Faust region has the added complexity of pre-existing basement structures and multiple phases of rifting and deformation.

6.3 ROLE OF INHERITED REGIONAL STRUCTURE

The analysis of structural trends in the Capel and Faust basins suggests that the inherited pre-rift structural fabric may have been a significant control on basin evolution. During much of the Palaeozoic and Mesozoic, the eastern Gondwana margin experienced convergent tectonics and terrane accretion. What these pre-existing terranes were composed of in the Lord Howe Rise region is still contentious, with recent work by Norvick et al. (2008), Mortimer et al. (2008) and Sutherland (1999) offering alternative scenarios. Most workers agree that the New England Orogen is likely to extend into the northern part of the Lord Howe Rise in the vicinity of the Capel and Faust basins. In addition, Norvick et al. (2008) suggests the possible extension of the Jurassic–Upper Cretaceous Clarence–Moreton and/or Maryborough Basin equivalents into the area. Seismic data over the Capel and Faust basins indicate the presence of a pre-rift sedimentary succession (‘layered’ basement; Colwell et al., 2010) beneath the deeper depocentres, which may represent these sedimentary rocks.

Irrespective of the basement terrane composition beneath the Capel and Faust basins, an overall NW–SE regional structural trend has previously been recognised over the Lord Howe Rise by a number of workers, particularly in potential field data (Sutherland et al., 1999; Willcox et al, 2001; Stagg et al., 2002; Schellart et al., 2006; Norvick et al., 2008; Collot et al., 2009; Figure 27). This corresponds with the dominant structural trends in the western and eastern areas of the Capel and Faust basins. As discussed previously, the dominant N-trend in the central zone of the study area likely represents intra-rift faults formed during the Syn-rift 1 phase under an extensional vector oblique to the structural grain.

Tectonic reconstructions by Gaina et al. (1998) and Norvick et al. (2008) place the Capel and Faust basins to the east of the present-day northern New South Wales coast during pre-Tasman Sea times (Figure 28). Major structures in the nearby onshore New England Orogen (based on Geoscience Australia’s 1:5 M onshore geology map) clearly show a dominant NW–SE trend, which largely reflects the configuration of the Palaeozoic eastern Gondwana convergent margin. Thus, the dominant NW structural trend over the Lord Howe Rise, including the Capel and Faust basins, appears to be a part of the regional grain of the former eastern Gondwana margin. This supports the contention that the New England Orogen underlies a large portion of the Lord Howe Rise.

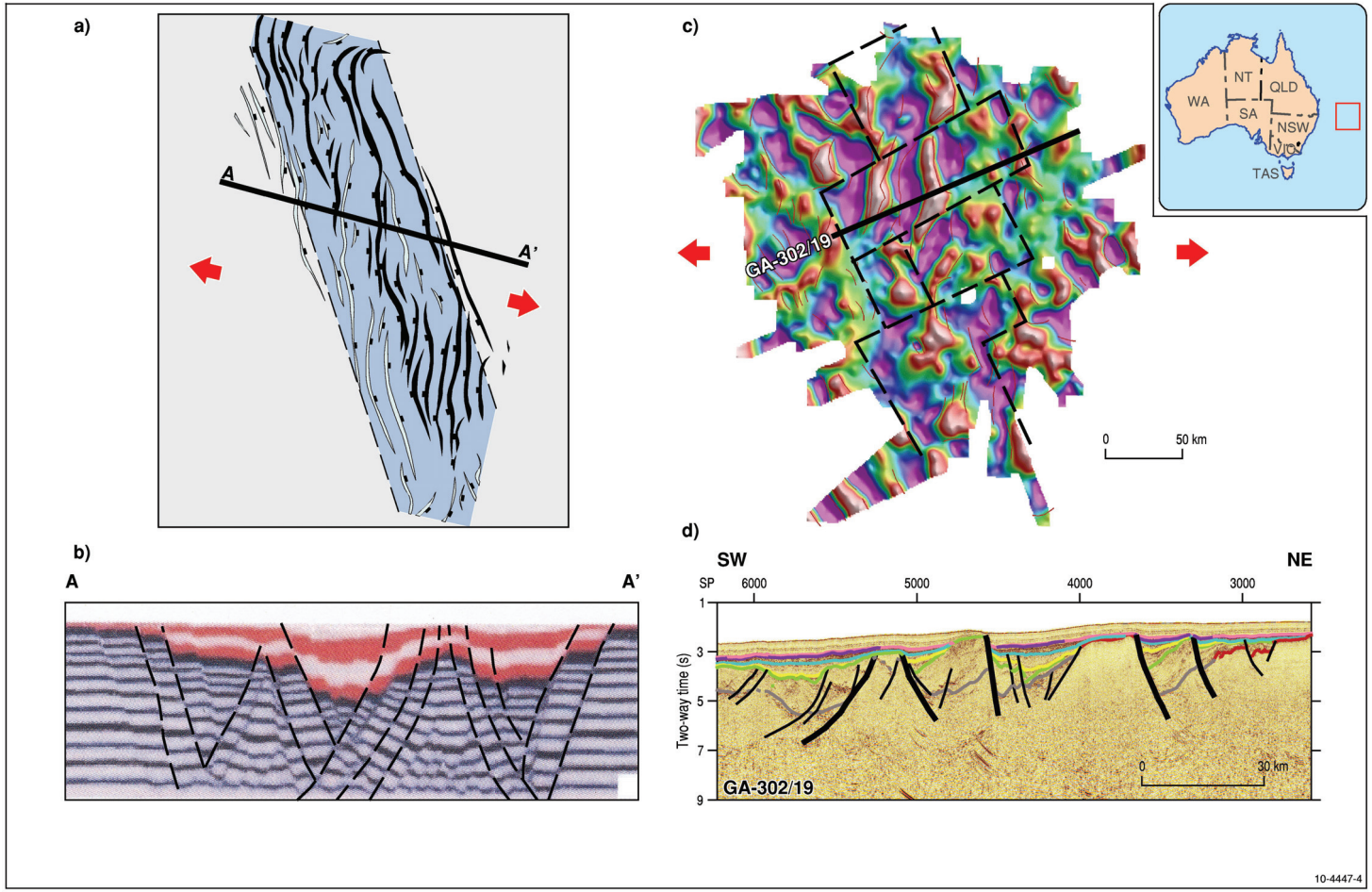

Figure 26: *(a) 60° oblique rift model line diagram interpretation after extension has ceased rotated for a pre-existing NW-trending fabric (after McClay et al., 2001) (b) Cross-section through the oblique rift model (after McClay et al., 2001). Line location on Figure 26a. (c) Bandpass-filtered Bouguer gravity with mapped major faults (shown in red) and structural zonation. The red arrows indicate the inferred rift extension vector (d) seismic cross-section of line GA-302/19. Line location shown in Figure 26c.*

Many other structural elements within the Lord Howe Rise and surrounding region appear to have utilised this NW-trending fabric. One example is the Vening–Meinesz Fracture Zone, which formed from the Early Miocene onwards with the development of the Norfolk Basin to the east (Herzer and Mascle, 1996). Van de Beuque et al. (2003**)** have suggested that a continuation of this feature crosses the Lord Howe Rise and the Capel-Faust area, terminating at the northern end of the Tasman Sea Basin**.** Gravity and magnetic data indicate that the extension of the fracture zone would coincide with the boundary between the western and the central structural zones within the Capel and Faust basins. The inferred age of rifting in the Capel and Faust basins is considerably older than that of the Vening–Meinesz Fracture Zone. This indicates that the latter structure, if it does continue through the Capel and Faust basins, has merely reactivated an earlier structure whose formation was controlled by the pre-rift structural grain.

6.4 PETROLEUM PROSPECTIVITY IMPLICATIONS

The 3D geological and geohistory modelling of the Capel and Faust basins confirm that the sediment thicknesses are sufficient for hydrocarbon generation within the largest depocentres in the central and northwestern areas of the basins (Funnell and Stagpoole, 2011; Hashimoto et al., 2011). Seismic character analysis, regional tectonic reconstructions and analogue basin studies suggest the likely presence of potential source rocks in the pre-rift, Syn-rift 1 and Lower Syn-rift 2 successions, potential reservoirs in the Upper Syn-rift 2 and Lower Post-rift successions, and regional seals in the Upper Post-rift section (Colwell et al., 2010 and Hashimoto et al., 2011).

3D modelling has also improved visualisation of the possible migration pathways and trapping structures present within the study area. The highly compartmentalised architecture of the depocentres would inhibit long-distance lateral migration of hydrocarbons away from the potential kitchen areas in the deeper parts of the depocentres, as well as encouraging multiple fragmented accumulations. Moreover, the occurrence of major syn-depositional bounding faults in proximity of the kitchen areas and the presence of multiple accommodation or relay zones may have encouraged vertical hydrocarbon migration at an early stage. Basin modelling indicates that, given the inferred pre-Late Cretaceous age of most potential source rocks that may be present in the area, a large part of hydrocarbon generation and migration would take place during the Cretaceous and early Cenozoic (Funnell and Stagpoole, 2011; Hashimoto et al., 2011). This would predate the last major structuring event (Eocene–Oligocene) and deposition of the potential regional seal (calcareous ooze and chalk) in the Upper Post-rift succession (Funnell and Stagpoole, 2011; Hashimoto et al., 2011), implying a risk of up-fault and updip hydrocarbon escape. The 3D geological model does indicate that structuring events following the syn-rift phases have resulted in the inversion and erosional truncation of syn-rift sediments in places along the margins of major depocentres, and that the final deposition of potential seals did not take place until well into the early Cenozoic. The 3D geological model also suggests that some anticlinal structures may have escaped breaching by erosion and thus preserve some of the early-generated hydrocarbons (Figure 29). Some of these features may constitute targets for further detailed investigation through data acquisition.

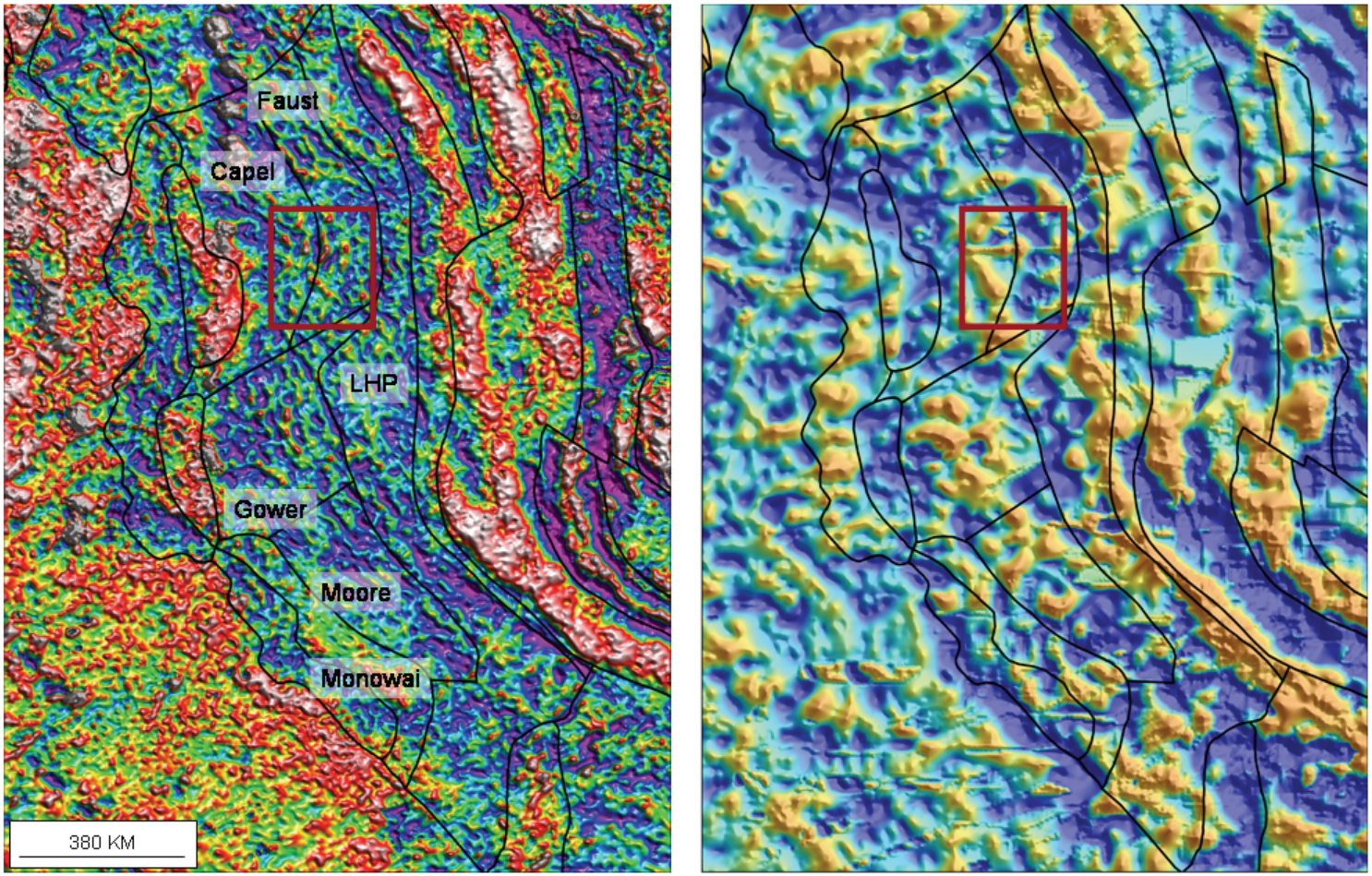

Figure 27: *Regional satellite-derived gravity (a) and magnetic (b) images showing the dominant NW-trending structural fabric of the Lord Howe Rise region. Study area shown in red outline. LHP = Lord Howe Platform.*

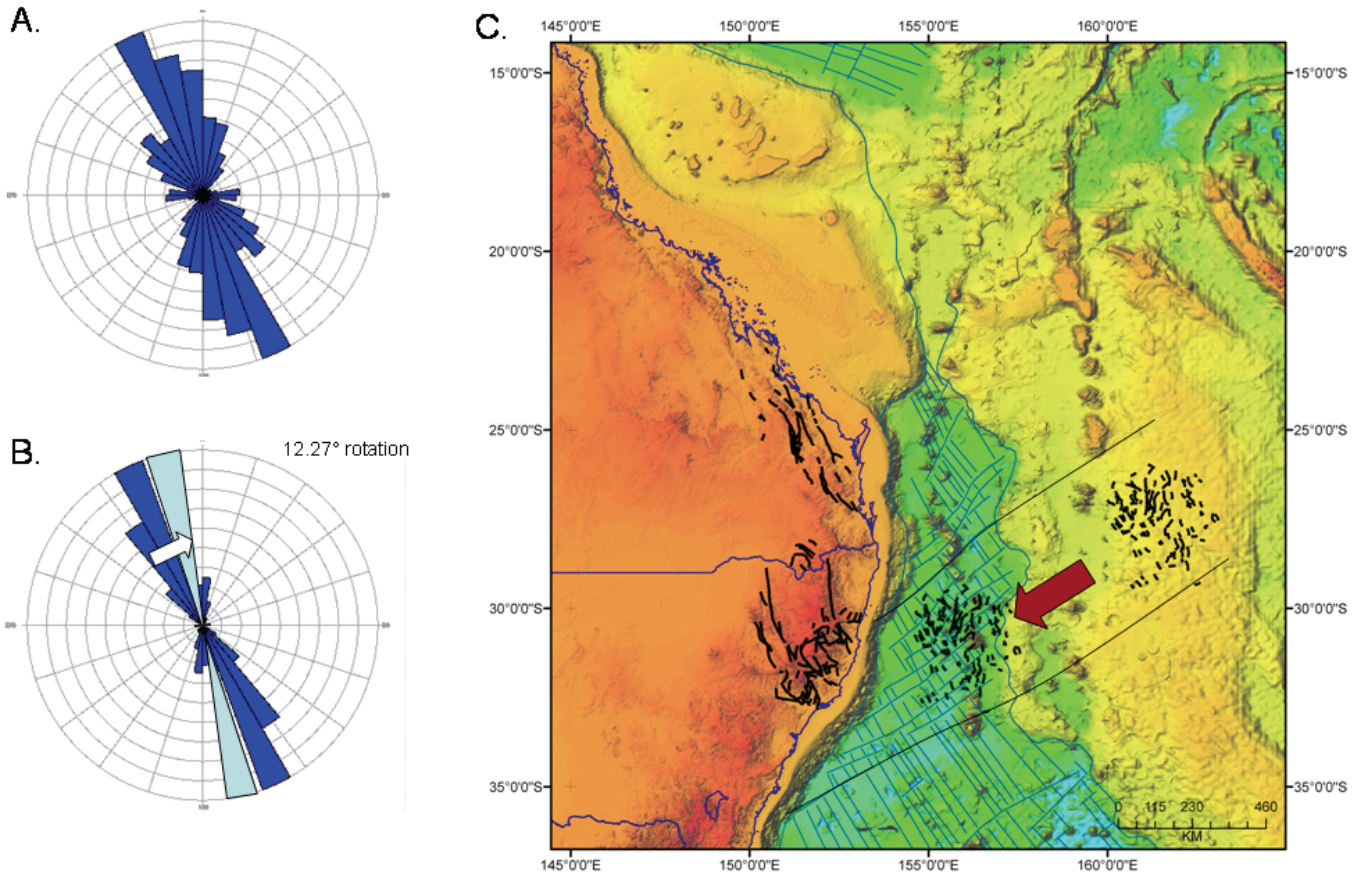

Figure 28: *Comparison of major fault trends in onshore eastern Australia and the Capel-Faust area. (a) Rose diagram of major fault strike trends in the New England Orogen extracted from 1:5M surface geology map by Geoscience Australia (1999) (b) Rose diagram of dominant fault strike trends in the eastern and western structural zones of the Capel and Faust basins. The light blue plot represents the fault trends after subtraction of the angle of rotation (c. 12° anticlockwise) resulting from the opening of the Tasman Sea (Gaina et al., 1998). (c) Location map of major faults in the New England Orogen and the Capel and Faust basins. The approximate pre-Tasman Sea location of the Capel and Faust faults, based on Gaina et al.(1998) and Norvick et al. (2008), is also indicated (red arrow).*

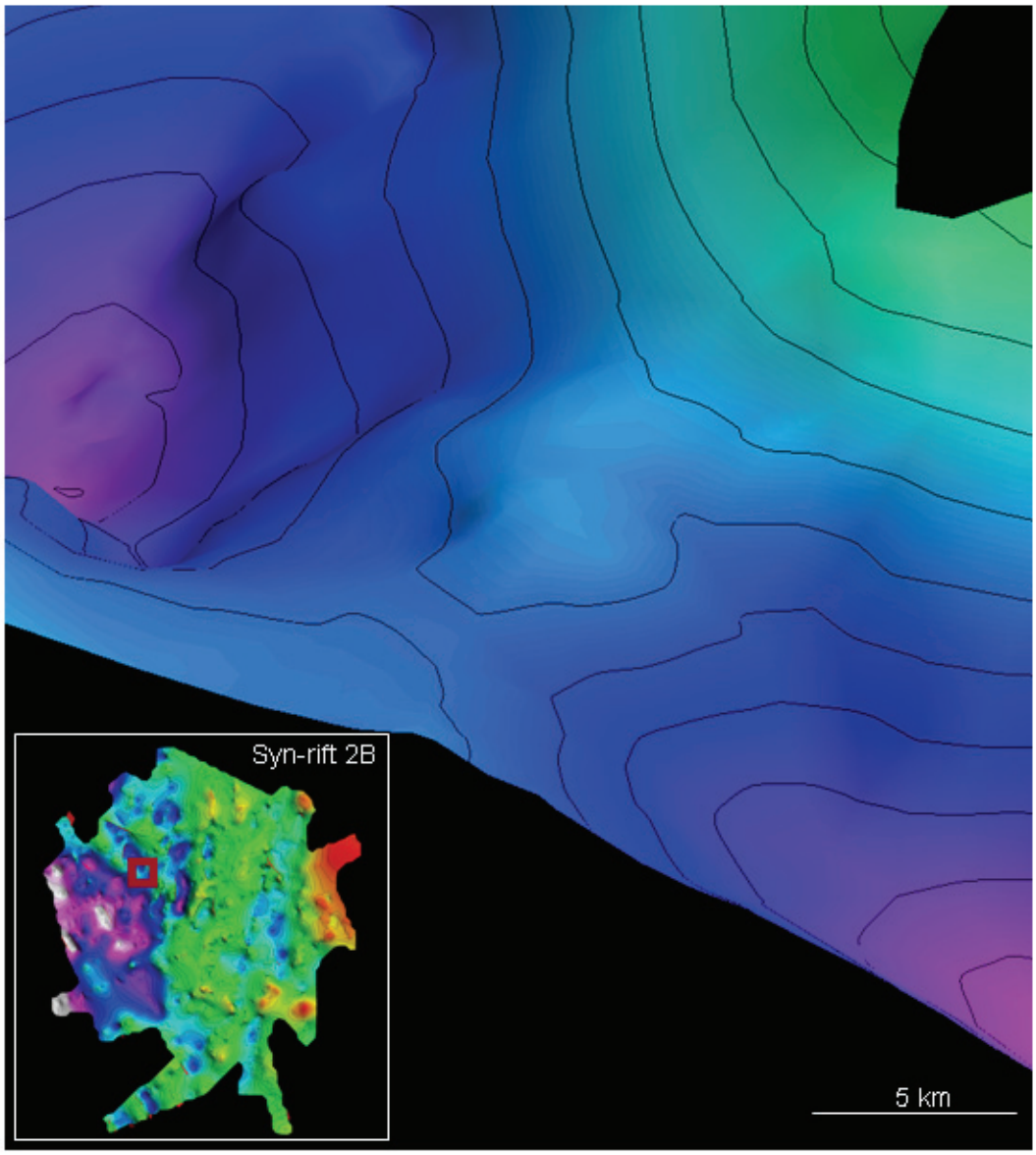

Figure 29: *Anticlinal structure at Top Syn-rift 2B surface that may potentially trap late-generated hydrocarbons.*

6.5 REGIONAL IMPLICATIONS

The acquisition of new high-quality geophysical data and 3D modelling have enabled the structure of the Capel and Faust basins to be analysed and interpreted at a greater level of detail, allowing further refined assessments of the basins' petroleum prospectivity. Regional satellite gravity data suggests that the structural configuration of the Gower Basin on the central Lord Howe Rise is superficially similar to that in the Capel and Faust basins. The presence of NNE-trending depocentres within an overall NW-trending grain appears duplicated in the Gower Basin, but it is offset dextrally along its northern boundary by the Barcoo–Elizabeth–Fairway lineament, a continuation of one of the Tasman Sea transform faults (Figure 27a) that has produced structural offsets as far eastward as the New Caledonia Basin (Van de Beuque et al., 2003).

Previous work by Willcox and Sayers (2001) in the Gower Basin defined two major syn-rift successions, based on interpretation of poorer quality seismic data (surveys 36A and 46), with a maximum sediment thickness of ~6.1 km. The depocentres also display similar dimensions to the Capel and Faust basins, at up to 20–40 km wide and 100–150 km long (Figure 27a). Given the similarities, it is likely that the Gower and Capel-Faust basins essentially formed under the same tectonic regime and that the Capel-Faust 3D model could be applied to the Gower Basin to infer its depocentre architecture and petroleum prospectivity.

Basins on the southern Lord Howe Rise, such as the Moore and Monowai basins, have a strong NW–trending gravity fabric with little evidence of N-trending depocentres (Figure 27a). It is likely these basins formed under a slightly different tectonic regime and/or inherited structural constraints. Gaina et al. (1998) distinguished this part of the Lord Howe Rise as a separate microcontinent region from the northern and central parts. As such, the Capel-Faust 3D model may not provide a suitable analogue for their structure, stratigraphy and associated prospectivity. Therefore, new data acquisition would be recommendable for a detailed geological and prospectivity assessment of the southern Lord Howe Rise basins.

7. Acknowledgements

The authors gratefully acknowledge the scientific inputs to the project by Richard Blewett, George Gibson, Paul Henson, Julianna Lockwood, Malcolm Nicoll, Graham Logan and Nadège Rollet (Geoscience Australia), and Ian Neilson (Jigsaw Geoscience). The constructive reviews of this report by Richard Blewett, George Gibson, Paul Henson and Richard Chopping (Geoscience Australia), and Ian Neilson (Jigsaw Geoscience) are also acknowledged.

8. References

Andrews, J.E., 1973. Correlation of seismic reflectors. *In:* Burns R.E., Andrews, J.E. et al. (Eds), *Initial Reports of the Deep Sea Drilling Project* **21**, US Government Printing Office, Washington, 459–479.

Archibald, N., Gow, P. and Boschetti, F., 1999. Multiscale edge analysis of potential field data. *Exploration Geophysics*, **30(2)**, 38–44.

Blevin, J.E., 2001. Hydrocarbon prospectivity of Australia's remote frontier areas in offshore east and southeast Australia – examples from the basins of Lord Howe rise. *In:* Hill, K.C. and Bernecker, T. (Eds), Eastern Australasian Basins Symposium; a refocussed energy perspective for the future, *Petroleum Exploration Society of Australia Special Publication*, 25–35.

Burns, R.E. and Shipboard Party, 1973. Site 208. *In:* Burns R.E., Andrews, J.E. et al. (Eds), *Initial Reports of the Deep Sea Drilling Project* **21**, US Government Printing Office, Washington, 271–331.

Collot, J., R. Herzer, Y. Lafoy, and L. Géli, 2009. Mesozoic history of the Fairway–Aotea Basin: Implications for the early stages of Gondwana fragmentation. *Geochemistry Geophysics Geosystems,* **10**, Q12019, doi:10.1029/2009GC002612.

Colwell, J., Foucher, J.-P., Logan, G. and Balut, Y., 2006. Partie 2, Programme AUSFAIR (Australia–Fairway basin bathymetry and sampling survey) Cruise Report. In: *Les rapports de campagnes à la mer, MD 153/AUSFAIR–ZoNéCo 12 and VT 82/GAB on board R/V Marion Dufresne*, Institut Polaire Français Paul Emile Victor, Plouzané, France, Réf : **OCE/2006/05**, 57–132.

Colwell, J. B., Hashimoto, T., Rollet, N., Higgins, K., Bernardel, G. and McGiveron, S., 2010. Interpretation of Seismic Data, Capel and Faust Basins, Australia's Remote Offshore Eastern Frontier. *Geoscience Australia Record* **2010/06**, 58pp.

Dadd, K.A., Locmelis, M., Higgins, K. and Hashimoto, T., 2011. Cenozoic volcanism of the Capel-Faust basins. *Deep Sea Research Part II: Topical Studies in Oceanography*, **58 (7–8)**, 922–932, doi: 10.1016/j.dsr2.2010.10.048.

Exon, N.F., Quilty, P.G., Lafoy, Y., Crawford, A.J. and Auzende, J-M., 2004. Miocene volcanic seamounts on northern Lord Howe Rise: lithology, age and origin. *Australian Journal of Earth Sciences*, **51 (2)**, 291–300.

Funnell, R. and Stagpoole, V., 2011. Petroleum systems models for Capel and Faust basins, eastern offshore Australia. *GNS Science Report prepared for Geoscience Australia*.

Gaina, C., Műller, D.R., Royer, J-Y., Stock, J., Hardbeck, J. and Symonds, P., 1998. The tectonic history of the Tasman Sea: a puzzle with 13 pieces. *Journal of Geophysical Research*, **103 (B6)**, 12413–12433.

Geoscience Australia, 2006. *GEODATA TOPO 250K Series 3*. Geoscience Australia, Canberra.

Hackney, R., 2010. Potential field data covering the Capel and Faust Basins, Australia's Remote Offshore Eastern Frontier. *Geoscience Australia Record* **2010/34**, 40pp.

Hashimoto, T., Higgins, K.L., Rollet, N., Stagpoole, V., Petkovic, P., Colwell, J.B., Hackney, R., Logan, G.A., Funnell, R. and Bernardel, G., 2011. Geology and prospectivity of the Capel and Faust basins in the deepwater Tasman Sea region. *APPEA Journal and Conference Proceedings*, **51**, Extended Abstracts.

Hashimoto, T., Rollet, N., Earl, K. and Bernardel, G., 2008. Capel and Faust basins — new information from the offshore frontier between Australia, New Zealand and New Caledonia. In: *2008 New Zealand Petroleum Conference Proceedings*, Crown Minerals, Ministry of Economic Development, Wellington.

Heap, A.D, Hughes, M., Anderson, T., Nichol, S., Hashimoto, T., Daniell, J., Przeslawski, R., Payne, D., Radke, L. and Shipboard Party, 2009. Seabed Environments and Subsurface Geology of the Capel and Faust basins and Gifford Guyot, Eastern Australia. *Geoscience Australia Record* **2009/22**, 167pp.

Herzer, R.H. and Mascle, J., 1996. Anatomy of a continent-backarc transform – The Vening Meinesz Fracture Zone Northwest of New Zealand. *Marine Geophysical Researches*, **18**, 401–427.

Hayes, D. E. and Ringis, J. 1973. Seafloor spreading in the Tasman Sea. *Nature*, **243**, 454–458.

Higgins, K., Hashimoto, T., Fraser, G., Rollet, N. and Colwell, J., 2011. Ion microprobe (SHRIMP) U-Pb dating of Upper Cretaceous volcanics from the northern Lord Howe Rise, Tasman Sea. *Australian Journal of Earth Sciences*, **58**, 195–207.

Hornby, P., Boschetti, F. and Horowitz, F.G., 1999. Analysis of potential field data in the wavelet domain. *Geophysical Journal International*, **137 (1)**, 175–196.

Jongsma, D. and Mutter, J.C., 1978. Non-axial breaching of a rift valley: evidence from the Lord Howe Rise and the Southeastern Australian margin. *Earth and Planetary Science Letters*, **39**, 226–234.

Krassey, A.A., Cathro, D.L. and Ryan, D.J., 2004. A regional tectonostratigraphic framework for the Otway Basin. *In:* Boult, P. J., Johns, D. R. and Lang, S. C. (Eds), Eastern Australasian Basins Symposium II, *Petroleum Exploration Society of Australia Special Publication*, 97–116.

Kroh, F., Morse, M.P. and Hashimoto, T., 2007. New data on the Capel and Faust basins. *Preview*, **130**, 22–24.

McClay, K.R., Dooley, T., Gloaguen, R., Whitehouse, P. and Khalil, S., 2001. Analogue modelling of extensional fault architectures: Comparisons with natural rift fault systems. *In:* Hill, K.C. and Bernecker, T. (Eds), Eastern Australasian Basins Symposium; a refocussed energy perspective for the future, *Petroleum Exploration Society of Australia Special Publication*, 573–586.

McDougall, I., Embleton, B. J. J. and Stone, D. B., 1981. Origin and evolution of Lord Howe Island, Southwest Pacific. *Journal of the Geological Society of Australia*, **28**, 155–176.

Milligan, P.R., Lyons, P. and Direen, N.G., 2003. Spatial and directional analysis of potential field gradients: new methods to help solve and display three-dimensional crustal architecture, *ASEG Extended Abstracts* **2003(2)**, doi:10.1071/ASEG2003ab108

Mortimer, N., Hauff, F. and Calvert, A.T., 2008. Continuation of the New England Orogen, Australia, beneath the Queensland Plateau and Lord Howe Rise. *Australian Journal of Earth Sciences*, **55 (2),** 195–209.

Norvick, M.S., Smith, M.A. and Power, M.R., 2001. The plate tectonic evolution of eastern Australasia guided by the stratigraphy of the Gippsland Basin. *In:* Hill, K.C. and Bernecker, T. (Eds), Eastern Australasian Basins Symposium; a refocussed energy perspective for the future, *Petroleum Exploration Society of Australia Special Publication*, 15–24.

Norvick M.S., Langford R.P., Hashimoto T., Rollet N., Higgins K.L. and Morse, M.P., 2008. New insights into the evolution of the Lord Howe Rise (Capel and Faust basins), offshore eastern Australia, from terrane and geophysical data analysis. *In:* Blevin, J.E., Bradshaw, B.E. and Uruski, C. (Eds), Eastern Australasian Basins Symposium III: Energy security for the 21st century, *Petroleum Exploration Society of Australia Special Publication*, 291–310.

Pepper, A.S. and Corvi, P.J., 1995a. Simple kinetic models of petroleum formation. Part 1: oil and gas generation from kerogen. *Marine and Petroleum Geology*, **12**, 291–319.

Pepper, A.S. and Corvi, P.J., 1995b. Simple kinetic models of petroleum formation. Part III: Modelling an open system. *Marine and Petroleum Geology*, **12**, 417–452.

Petkovic, P., 2010. Seismic velocity models of the sediment and upper crust of the Capel and Faust Basins, Lord Howe Rise. *Geoscience Australia Record* **2010/03**.

Schellart, W.P., Lister, G.S. and Toy, V.G., 2006. A Late Cretaceous and Cenozoic reconstruction of the Southwest Pacific region: tectonics controlled by subduction and slab rollback processes. *Earth-Science Reviews*, **76**, 191–233.

Shor, G.G., Kirk, H.K. and Menard, G.L., 1971. Crustal structure of the Melanesian arc. *Journal of Geophysical Research*, **76**, 2562–2586.

Slater, R.A. and Goodwin, R.H., 1973. Tasman Sea guyots. *Marine Geology*, **14**, 81–99.

Stagg, H.M.J., Alcock, M.B., Borissova, I. and Moore, A.M.G., 2002. Geological framework of the southern Lord Howe Rise and adjacent areas. *Geoscience Australia Record* **2002/25**, 104pp.

Stagg, H.M.J., Borissova, I., Alcock, M. and Moore, A.M.G., 1999. Tectonic provinces of the Lord Howe Rise; Law of the Sea study has implications for frontier hydrocarbons. *AGSO Research Newsletter*, **31**, 31–32.

Sutherland, R., 1999. Basement geology and tectonic development of the Greater New Zealand region: an interpretation from regional magnetic data. *Tectonophysics*, **308**, 341–362.

Van de Beuque, S., Stagg, H.M.J., Sayers, J., Willcox, J.B. and Symonds, P.A., 2003. Geological framework of the northern Lord Howe Rise and adjacent areas. *Geoscience Australia Record* **2003/01**, 92pp.

Webster, M. and Petkovic, P., 2005. Australian bathymetry and topography grid, June 2005. *Geoscience Australia Record* **2005/12**.

Wessel, P. and Smith, W.H.F., 1991. Free software helps map and display data. *EOS*, **72**, 441.

Willcox, J.B. and Sayers, J., 2001. Gower Basin, Lord Howe Rise *In:* Hill, K.C. and Bernecker, T. (Eds), Eastern Australasian Basins Symposium: a refocused energy perspective for the future, *Petroleum Exploration Society of Australia Special Publication*, 189–201.

Willcox, J.B., Sayers, J., Stagg, H.M.J. and Van de Beuque, S., 2001. Geological framework of the Lord Howe Rise and adjacent oceanic basins. *In:* Hill, K.C. and Bernecker, T. (Eds), Eastern Australasian Basins Symposium: a refocused energy perspective for the future, *Petroleum Exploration Society of Australia Special Publication*, 211–225.

Zhu, H. and Symonds, P.A., 1994. Seismic interpretation, gravity modelling and petroleum potential of the southern Lord Howe Rise region. In: *1994 New Zealand Petroleum Conference Proceedings*, Ministry of Commerce, Wellington, 223–230.

Appendix 1: Model Building Tools

Unless otherwise stated all command listed refer to GOCAD version 2.5.2

A1.1 BASIC DATA

A1.1.1 Cultural

The cultural data in this 3D model refers to the Australian EEZ and coastline boundaries. This data was obtained as an ARCGIS shapefile and imported in as a Curve file.

STEP 1: IMPORT SHAPEFILE
File-Import Objects-Cultural Data-Cultural Data-Arcview Shape

A1.1.2 Bathymetry

Bathymetry data can be loaded as both images (GeoTIFFS) and as grids. Draping high resolution bathymetry images onto low resolution surfaces can provide high quality bathymetric information while avoiding data dense layers.

Capel-Faust Bathymetry

STEP 1: IMPORT GEOTIFF
File-Import Objects-Images-Georeferenced Images-GeoTIFF Image
Image file is loaded as a voxet into GOCAD™

STEP 2: SEAFLOOR DRAPE
Right click on seafloor surface file in the catalogue tree
Select 'Attributes'
Under the 'Texture' tab, in the 'Draping' section
Select 'Visible'
Navigate to the bathymetry image voxet

Regional Bathymetry

STEP 1: IMPORT ZMAP GRID
Right click on 2D-Grid
New-Import from-ZMAP ASCII

STEP 2: BUILD SURFACE FROM 2D-GRID
Right click on 'Surface' heading in the catalogue tree menu
New-From 2D-Grid

A1.1.3 Wells

Wells can be loaded individually or in batches within GOCAD™ if naming conventions are consistent. Editing the data files, including any depth to time conversion, will make the well loading more efficient. Well paths, age markers and logs can be loaded and displayed.

STEP 1: EDIT BASIC DATA FILES
Clean up data files so that formats and naming conventions are consistent allowing for batch loading. If needed, convert depth values to time

STEP 2: LOAD WELL PATH
A well path needs to be loaded for each well that designates the well start and total depth, as well as any deviation in the hole.
Right click on the 'Well' heading in the catalogue tree.
New-Import from-Column-based File

STEP 3: LOAD AGE MARKERS
Expand the 'Well' heading in the catalogue tree.
Expand the new well file in the catalogue tree.
Right click on the 'markers' heading for the well file.
Import from-Column-based File

STEP 4: LOAD LOGS
Expand the 'Well' heading in the catalogue tree.
Expand the new well file in the catalogue tree.
Right click on the 'logs' heading for the well file.
Import from-Column-based File

A1.1.4 Seismic

STEP 1: IMPORT SEGY FILES
Seismic SEGY files are imported into GOCAD™ and converted to voxet files. Each seismic line was loaded individually.

Right click on the 'Voxet' heading in the catalogue tree.
New-Import from-SEG-Y-2D

STEP 2: REMOVE UN-NEEDED SECTIONS
Many of the voxet seismic lines contain large amounts of water column information, as well as deep seismic data where visualisation is very poor. By removing these un-needed sections the seismic file size is further reduced aiding processing time.

In voxet mode, New-Extracted From Voxet

STEP 3: REDUCE RESOLUTION
An extract of the voxet file is taken to reduce file size and display time for the seismic data. In this project the seismic data was sub-sampled to a third of its original resolution.

In voxet mode, New-Extracted From Voxet

STEP 4: WATER COLUMN TRANSPARENCY
After removing large sections of water column from the seismic voxet files, any remaining water column can be made transparent. This greatly improves seismic data visualisation. This is achieved by copying the seafloor horizon, moving it slightly higher than the seafloor (to avoid removing any of it) and using this surface to create a water column region on the seismic lines. This region is then assigned a null value on the seismic traces property (in this case represented by 'seismic') and can be set to transparent. Note: The seafloor surface used to create the water column region must cover the extents of the seismic files.

Create a new region
Expand voxet file in catalogue tree
Right click on regions-Create from Geologic Feature
Select seafloor horizon (that has been adjusted slightly above the seafloor) as the base of the region

Assign null value to water column region
Expand seismic file in catalogue tree
Right click on 'property'
Select 'Apply Script'
Make sure the water column region is selected.
Apply the following script 'seismic=-99999'

Set null value to transparent
Expand seismic file in catalogue tree
Expand 'property'
Right click on seismic traces property 'seismic'
Select 'Attributes'
On the 'Property' tab
Select 'Use no data value'
Set 'Transparency' to 1 and click 'Apply'
Water column region is now transparent

A1.1.5 Potential field

STEP 1: IMPORT POTENTIAL FIELD ZMAP GRIDS AS 2DGRID

Right click on the '2D-Grid' heading in the catalogue tree.
New-Import from-ZMAP ASCII

STEP 2: CONVERT 2D-GRID TO A SURFACE

In surface mode
New-From 2D-Grid-Entire 2D-Grid

STEP 3: IMPORT GEOTIFF
Import high resolution georeferenced image with appropriate sun shading or image enhancements.

File-Import Objects-Images-Georeferenced Images-GeoTIFF Image

STEP 4: DRAPE GEOTIFF

Right click on potential field surface file in the catalogue tree
Select 'Attributes'
Under the 'Texture' tab, in the 'Draping' section
Select 'Visible'
Navigate to the potential field image voxet

A1.2 INTERPRETIVE DATA AND MODEL BUILDING

A1.2.1 Horizons

STEP 1: SCHLUMBERGER GEOFRAME™ HORIZON INTERPRETATION
Horizons interpreted on S302 and GA-206 seismic surveys. Data export in ASCII format from Data Manager.

STEP 2: GOCAD™ POINTSSETS IMPORT AND EDITING
Import
File-Import Objects-Horizon Interpretations-PointsSets-Column-based File

Removing bad data points: Bad data values in the original import files may place points outside of the study area. To remove these points the following commands were used.

Create a new region
PointsSet mode-Region-Region Editor
Select 'new' button
Select points within study area
Delete points outside of region
PointsSet mode-Tools-Region-Keep Points

Filtering the PointsSet: The amount of points imported into the project may be more data dense than necessary. PointsSets in this dataset were reduced to roughly a third of their original amount, approximately 50,000 points.

Filter a PointsSet to 50,000 points
Right click on PointsSet file to bring up menu.
Edit-Filter
Max points: 50000
Partitionner Criterion: Number of points

STEP 3: PETROSYS GRIDDING AND EXPORT
Gridding Parameters
Cell Size: 5 km
Seismic Lines: s302, 206r
Operation: Standard gridding
Algorithm: Minimum curvature
Interpolation: Bicubic
Clipped to s302 seismic line extents

Export
Gridding and Contouring
File-Export-Zmap-Grids

STEP 4: GOCAD™ 2D-GRID IMPORT, CONVERSION, CONTROL POINTS AND CONSTRAINTS
Importing Petrosys ZMAP ASCII files
Right click on '2D-Grid' heading in the catalogue tree menu
Import from-ZMAP ASCII

2d Grid to Surface Conversion
Right click on 'Surface' heading in the catalogue tree menu
New-From 2D-Grid

Set Control Points on Surface: Sets seismic interpretation points as a control on an appropriate surface. Any interpolations or editing on the surface will try to match the location of these points.

Click on PointsSet
Drag onto surface file in the Catalogue tree
Select 'Set as Control Points'

Set Border Constraints on Surface: Sets constraints on the surfaces outer border so that any interpolations on the surface adjusts the surface up and down, rather than shrinking and expanding.

Surface mode-Constraints-New-Constraint on Border-Set On Straight Line-All Borders
Select horizon
Tick 'Force direction'
Set 'Dir_shoot' X=0 Y=0 Z=1

STEP 5: GOCAD™ HORIZON SURFACE EDITING
Beautify Triangles: Improves the appearance of a horizon surface by removing poorly shaped triangles.

Surface mode-Tools-Beautify-Beautify triangles for equilaterality

Decimate*:* Controls the resolution of triangles based on slope. For smooth flat areas less triangles are needed, for rugose topography more triangles are needed.

Surface mode-tools-decimate

Node Editing*:* Individual nodes on a triangle may be adjusted. Any subsequent interpolations run on the surface will capture and integrate this change. A region can be created surrounding the node and interpolations can be run within this area only, rather than applied to the whole surface

Move nodes
Surface mode-tools-node

Set control node
Surface mode-constraints-Control Nodes-Set-One

Run interpolation
Right click on surface file-Fit Geometry

Run interpolation in region
Surface mode-Interpolation-Geometry-In Region

Isopach Maps*:* Once gridded surfaces have been created, thickness between the units can be readily calculated and displayed on the surface as a surface property.

Calculate Unit Thickness
Surface mode-Compute-Property-Compute Vertical Thickness
Surface: Surface of interest
Thickness: New property name (e.g. isopach_to_wb)
Surface Bottom: Surface control for calculating thickness. May be top or bottom.

Display Unit Thickness
Expand surface file display
Expand 'properties'
Select new thickness property

Horizon Surface Resolution Optimisation: Adjusts horizon resolution based on the average error of the horizon surface to the base interpretation (control points). GOCAD version 2.1.6.

Surface mode-Edit-Optimise
Criteria: Control points using average error
Min-Max: Select value between 0 to 100%

Constraints:

Range Thickness Constraints: Uses the thickness relationship between surfaces to constrain surface interpolation by having a maximum and a minimum allowed thickness.

View Unit Thickness
Expand surface file display
Expand 'properties'
Right click on unit isopach thickness property
Compute-Histogram
Set minimum thickness constraint to slightly more than 0 to avoid any horizon surface overlap
Use maximum isopach thickness to define maximum thickness constraint

Set Range Thickness Constraints
Surface mode-Constraints-Set Range Thickness Constraint
Select two surfaces
Enter minimum and maximum allowed thickness between the two surfaces

Veclink: Used to help visualise fault movement on surfaces. Produces a series of lines joining the fault top border to the fault bottom border.

Surface mode-Constraints-Constraints on Border-Set Veclink

A1.2.2 Faults

STEP 1: SCHLUMBERGER GEOFRAME™ FAULT INTERPRETATION
Faults interpreted on S302 and GA-206 seismic surveys. Data export in ASCII format from Data Manager in GeoFrame.

STEP 2: GOCAD™ FAULT IMPORT
CURVES IMPORT
File-Import Objects-Fault Interpretations-Fault Sticks (Curves)-Column-based File

STEP 3: FAULT SURFACE INTERPRETATION
Create a fault curve map file that links appropriate fault curves from the seismic interpretation. The fault curve map file must intersect with the tops of the seismic cross-section faults to build surfaces using 'Geological Toolbox'.

Right click on 'Curve' heading in catalogue tree
New-From Digitized Polyline

STEP 4: FAULT SURFACE BUILDING
Build fault surfaces using a fault curve map and seismic fault cross-section curves. If no cross-section curves are available determine appropriate dip and fault length value manually.

In 'Geological Toolbox' mode

Fault Builder-
New fault from line or dip
New fault from line and one xsection
New fault from line and several xsections

STEP 5: FAULT ORIENTATIONS
Fault orientation data was generated using a script and a wizard provided by Jigsaw Geoscience and Mira Geoscience producing a PointsSet ('Fault_Orientation_Data') where orientation is captured as a vector property encapsulating the fault orientation, dip and dip direction. This created a data point for each triangle node on the fault surfaces. This PointsSet was edited so that only central points were used. For small faults only one orientation data point was captured. For larger faults, with changes in orientation along length, a number of data points were used. A 'dip_direction' property was also added manually to the fault surfaces file to capture major changes in east and west dipping faults. This property was displayed as colours on the fault surfaces.

Orientation PointsSet Editing
Create a new region to capture unwanted orientation points
Curve mode-Region-Region Editor
Select "new" button
Select points

Delete unwanted orientation points
PointsSet mode-Tools-Region-Delete Points

Dip direction for fault surfaces
Create a new Dip direction property for fault surfaces
Expand file in catalogue tree
Right click on properties-Create

Create a new region to capture east/west dipping faults
Surface mode-Region-Region Editor
Select “new” button
Select east/west dipping faults

Assign values to new ‘Dip_direction’ property based on gross dip (e.g. west-dipping = 1, east-dipping= 0)
Expand fault surfaces file in catalogue tree
Right click on properties-Apply Script
Select east/west dipping fault region
Apply script: Dip_direction = ‘1’ or Dip_direction = ‘0’

Display east/west dipping faults
Expand fault surfaces file in catalogue tree
Expand properties
Select ‘Dip_direction’

A1.2.3 Horizon-Fault Integration

STEP 1: FAULT-HORIZON CUT
Cut holes in horizon surfaces around fault surfaces.

Create a new surface part
In the Digitization/Editing toolbar
Set to Surface mode
Use 'Cut Surface by Scissor Polygon' to create a new surface part around the fault surface

Remove new part around fault surfaces
Surface mode-Tools-Part-Delete Selection

STEP 2: SET CONSTRAINTS
Once a hole is cut into a horizon surface the edge of the hole becomes a surface border. This border is then assigned the fault surface as a constraint, effectively telling the border to move towards the fault surface to create sealed surfaces.

Surface mode-Constraints-Constraints on Border-Set on Surface

STEP 3: SET BORDER REGION
The horizon surface fault hole border nodes are assigned to a region so that an interpolation will only affect the hole edges, rather than the whole surface.

Create a new region
Surface mode-Region-Region Editor
Select 'new' button

Set border nodes to new region
Surface mode-Region-From Border

STEP 4: FAULT-HORIZON SEAL
An interpolation is run on the horizon surface hole borders to align them with the fault surfaces, creating fault sealed horizons.

Surface mode-Interpolation-In Region

STEP 5: FAULT MOVEMENT
Total fault movement can be captured and visualised for every horizon surface. This is achieved by defining fault tops and bottoms by creating curves based on the horizons fault borders. The distance can be computed between these curves and captured as a property. Lastly a surface is created by using the fault top and bottom borders and the fault movement is painted onto this surface. By using the same colour ramp and scale on these surfaces fault movement can be compared across the region, for an individual horizon surface, or between multiple horizon surfaces.

Create fault top and bottom curves for a horizon surface
Curve mode-New-From Surfaces-Borders-One

Calculate distance between fault tops and bottoms and capture as a property on the fault bottom curve file
Mining Utilities-Utilities-Create/Edit GOCAD™ Object Properties-Compute Distance From Atomic Object-To Curve

AtomsSet Name: Fault_Bot
Curve Name: Fault_Top
Distance property name: Fault_Movement

Create fault movement surface joining fault tops and bottoms
Surface mode-New-From Surfaces-Borders-One

Paint fault movement surface with fault movement property
Surface mode-Property-Transfer Property-Paint Surface from Discrete Properties Points by Interpolation

Surface: fault movement surface
Points: Fault_bot curve
Property: Fault_Movement

A1.2.4 Depth Conversion

To convert datasets from the time to depth domain requires the creation of a velocity model that can be applied to the datasets. GOCAD™ allows the creation of velocity models which use both interval and algorithm velocity methods. Once a velocity model has been created both basic datasets and interpretative data can be readily converted.

STEP 1: GEOLOGICAL FEATURES
By assigning the horizon surfaces as geological features they may be used to define regions in a velocity model voxet. This enables the use of geological interval velocities.

In Surface mode
Edit-Set Geologic Information
Assign “Geologic feature” name
Assign “Geologic type”

STEP 2: VELOCITY MODEL VOXET
An empty velocity voxet model is constructed that encompasses all datasets, both basic data and interpretive. An appropriate resolution for the velocity model must be selected. A high resolution dataset may be inefficient for processing purposes. It was felt 200 nodes for U, V and Z axis was sufficient to capture regional velocity changes for this model.

In voxet mode
New-From Objects Cage
Select all seismic lines
Set number of nodes within voxet cage

STEP 3: CREATE REGIONS
The velocity model for the area can have velocity changes related to geological changes by using geological horizon surfaces to define regions within the velocity model. For this model it was decided to split the model into three main regions; a water column and two sedimentary regions which will have different velocity algorithms applied. It is advisable to extend surfaces used to define regions by a cell length to ensure that the velocity model data encompasses all of the projects data.

Create a new region
Expand velocity model voxet file in catalogue tree
Right click on regions-Create from Geologic Feature
Select seafloor horizon as the base of the region ‘water column’
Select seafloor horizon as the top of the region ‘sediment’

STEP 4: ASSIGN VELOCITIES
Create Velocity property
Expand velocity model voxet file in catalogue tree
Right click on ‘properties’
Select ‘Create’
Property Name: Velocity
Property Type
Category: Geophysics Type: Velocity

Assign Velocity algorithm to regions
Expand velocity model file in catalogue tree
Right click on properties-Apply Script
Select region
Apply script

STEP 5: AVERAGE VELOCITIES
A new ‘Average Velocity’ property is created using the assigned velocities. By averaging the velocities large changes in velocity are smoothed out to produce a better depth conversion result.

Create ‘Average Velocity’ property
Expand velocity model voxet file in catalogue tree
Right click on ‘properties’
Select ‘Create’
Property Name: Average Velocity
Property Type
Category: Geophysics Type: Velocity

Calculate ‘Average Velocity” using ‘Velocity’ property
In velocity mode
Select ‘Velocity Conversion’
Select ‘Voxet: In One Domain
Select velocity model voxet
Input Velocity Property: velocity
Velocity Type: two-way time interval
Output Velocity Property: Average Velocity
Velocity Type: two-way time average

STEP 6: DEPTH CONVERSION
In velocity mode
Select ‘Time-Depth Conversion’
Convert Objects Using Velocity
Select objects for conversion in ‘objects list’
Select Voxet Velocity cube
Average Velocity: Average velocity property
Velocity unit: m/s (two way time)
Select ‘Time to depth conversion’
Seismic reference datum: constant
Value: 0
Click ‘OK’